ABSTRACT

Title of Thesis:	NUTRIENT EFFECTS ON PHYTOPLANKTON COMMUNITY COMPOSITION IN THE EUTROPHIC ANACOSTIA RIVER AND A FOCUS ON DIATOM PHYSIOLOGY
	Samantha J. Gleich, Master of Science, 2019
Thesis Directed By:	Patricia M. Glibert, Professor Marine Estuarine Environmental Science

The Anacostia River, Washington D.C., is a freshwater ecosystem that historically received high concentrations of nutrients from sewage and stormwater outfalls. Restoration efforts have been implemented recently that may improve water quality and alter the relative abundance of different phytoplankton taxa in the river. To determine the effects that environmental shifts may have on diatom abundance and phytoplankton community composition in the Anacostia River, a mesocosm experiment and laboratory studies were conducted. The results of the mesocosm study revealed that diatoms were consistently outcompeted by cyanobacteria. Additionally, phosphorus enrichment led to a 50% increase in cyanobacterial abundance and decreased the abundance of diatoms. In the culture study, shifts in water temperature and nutrient availability altered diatom growth rates, photosynthesis, silica deposition, and NO_3^- reduction. Together, these studies highlight the interactive effects that nutrient availability and temperature may have on the physiology and subsequent growth of diatoms in the Anacostia River.

NUTRIENT EFFECTS ON PHYTOPLANKTON COMMUNITY
COMPOSITION IN THE EUTROPHIC ANACOSTIA RIVER AND A FOCUS
ON DIATOM PHYSIOLOGY

by

Samantha J. Gleich

Thesis submitted to the Faculty of the Graduate School of the
University of Maryland, College Park and University of Maryland Center for
Environmental Science, in partial fulfillment
of the requirements for the degree of
Master of Science
2019

Advisory Committee:
Professor Dr. Patricia M. Glibert, Chair
Associate Professor Dr. Louis V. Plough
Assistant Research Professor Dr. Greg Silsbe
Professor Dr. Caroline M. Solomon

Table of Contents

List of Tables

List of Figures

reproduced in each panel for reference.

Chapter 1: Nutrient effects on phytoplankton community composition in the eutrophic Anacostia River and a focus on diatom physiology: Introduction

The Anacostia River is a small tributary of Chesapeake Bay that begins in Bladensburg, Maryland, and flows through the District of Columbia. This eutrophic river system has faced a long history of neglect and was named one of the highest priority regions of concern within the Chesapeake Bay region in 2002 (CBP 2002). A major source of pollution to the Anacostia River has been the untreated sewage and stormwater effluent that enters the river from combined sewer overflow outfalls (CSOs) that are found along the water (Brandes 2005, Solomon et al. 2019). The polluted waters that are discharged into the Anacostia River from the CSOs are rich in nutrients and have likely contributed to the high ambient levels of nitrogen (N) that are found in the water column of this river in the modern-day (Solomon et al. 2019). Nutrients entering the river from the CSOs and from the surrounding urban use have helped fuel the high biomass and potentially harmful picocyanobacterial blooms that have been noted during summer months on the Anacostia River (Jackson 2016, Solomon et al. 2019).

In an attempt to improve the water quality and the overall health of the Anacostia River system, the District of Columbia Water and Sewer Authority implemented the Anacostia River Tunnel Project in March 2018. The Anacostia River Tunnel is an underground sewage and stormwater diversion tunnel that was designed to divert CSO effluent to the Blue Plains Wastewater Treatment Plant, thus preventing these polluted waters from being discharged directly into the Anacostia River (DC Water and Sewer Authority 2002). The implementation of this large-scale

restoration project should lead to reductions in nutrient-loading and changes in the

relative abundance of the different chemical forms of N, as CSO effluent is rich in

reduced N forms such as ammonium (NH_4^+) and urea as opposed to oxidized N forms

such as nitrate (NO_3^-; Solomon et al. 2019). Changes in the relative abundance of

NH_4^+ and NO_3^- have been associated with shifts in phytoplankton community

composition in a number of aquatic ecosystems (Berg et al. 2003, Dugdale et al.

2007, Domingues et al. 2011, Glibert et al. 2014, 2016, Shangguan et al. 2017). These

changes in community diversity under varying NH_4^+: NO_3^- conditions may be related

to the unique physiological capabilities that different phytoplankton functional groups

possess and may ultimately allow certain phytoplankton taxa to outcompete others as

the relative abundance of different N forms in the water column changes (Lomas and

Glibert 1999a,b, Parker and Armbrust 2005, Glibert et al. 2016).

One specific phytoplankton functional group that may be affected by changes

in the relative abundance of NH_4^+ and NO_3^- are the diatoms. Diatoms form the basis

of some of the most productive and efficient food chains in the world (Cushing 1979)

and are thought to prefer NO_3^- as an N source (Patrick 1948, Probyn and Painting

1985, Dortch 1990, Lomas and Glibert 1999a, b, Glibert et al. 2016). It has been

suggested that diatoms thrive under high NO_3^- conditions due to their relatively high

NO_3^- uptake rates, their ability to store large amounts of NO_3^- internally, and their

abundance of high-affinity NO_3^- transporters (Lomas and Glibert 1999b, Lomas and

Glibert 2000, Song and Ward 2007, Glibert et al. 2016 and references therein). In

addition to this documented preference for NO_3^-, diatom growth and NO_3^-

assimilation may decrease when NH_4^+ concentrations are high (Syrett and Morris

1963, Lomas and Glibert 1999a, Dugdale et al. 2007, Glibert et al. 2016). It has been documented that diatom abundance is inversely correlated with water NH_4^+ concentration in the Anacostia River (Solomon et al. 2019), suggesting that the high ambient NH_4^+ concentrations that have been noted in the Anacostia River may be affecting diatom growth and persistence at certain times throughout the year.

In addition to the effects that N abundance and form may have on diatom growth and physiology, other environmental factors that will not be affected by the implementation of the Anacostia River Tunnel Project, such as water temperature, may also influence the relative abundance of diatoms in an aquatic ecosystem. Diatoms are often the dominant phytoplankton group present during spring bloom events when waters are cool, nutrients are supplied to the phytoplankton in episodic pulses, and waters are weakly stratified (Cushing 1989, Goldman 1993, Lomas and Glibert 1999b). Water temperature has been shown to affect diatom NO_3^- assimilation (Lomas and Glibert 1999b) and cell silicon content in certain diatom species (Paasche 1980), suggesting that changes in temperature have the capacity to alter diatom physiology and may in turn lead to changes in diatom abundance. Specifically, cold (< 10 °C) and hot (>20 °C) temperature conditions may decrease the activity of the nitrate reductase (NR) enzyme that catalyzes the first step of NO_3^- reduction in algal cells (Lomas and Glibert 1999a,b, Berges et al. 2002, Gao et al. 2000). Additionally, colder water temperatures have been associated with increases in diatom cell wall silicification and increases in the silicon quota of specific diatom species (Liu and Glibert 2018, Lomas et al. 2019, Paasche 1980). These temperature-dependent processes may be regulated by imbalances in cellular metabolism that occur when

diatom cells are subject to stressful environmental conditions and may ultimately influence the growth and productivity of diatom cells in an aquatic ecosystem.

The Anacostia River is atypical in its seasonal bloom patterns compared to other temperate aquatic systems, in that spring diatom blooms do not attain a biomass as high as that of summer blooms (Solomon et al. 2019). This lack of diatom biomass accumulation that has been noted during the spring season on the Anacostia River may be related to environmental factors such as nutrient availability and water temperature. The implementation of the Anacostia River Tunnel Project will likely lead to increases in water quality over time and may, in turn, lead to changes in nutrient abundance and form, phytoplankton community composition, and the prevalence and succession of diatom communities. Therefore, the research herein aims to address the general hypothesis that nutrient abundance, nutrient form, and water temperature may synergistically influence diatom physiology and growth in the Anacostia River ecosystem. To determine the synergistic effects that these environmental shifts may have on diatom physiology and abundance, the following questions were addressed:

- How do high ambient NH_4^+ concentrations and water temperatures typical of the Anacostia River during the summer months impact phytoplankton community composition and the prevalence of diatoms in the Anacostia River?

- How do NO_3^- availability, silicate availability, and water temperature alter diatom growth rate, photosynthesis, and cell wall silicification?

- Do extreme temperature conditions alter the rate of NO_3^- reduction in Anacostia River phytoplankton communities and specifically that of diatom cells?

In order to address these questions, field and laboratory-based experiments were carried out. First, a mesocosm study was conducted on the Anacostia River to examine how enrichment with different nutrients may alter phytoplankton physiology and community composition (Chapter 2). Then, a series of culture-based studies were conducted using a model diatom species, *Thalassiosira pseudonana*, to determine how NO_3^- availability, silicate availability, and water temperature affect diatom growth and physiology (Chapter 3). Together, these studies begin to highlight the physiological responses of diatom cells to changes in the surrounding environment and how these responses may subsequently alter diatom growth and abundance in an aquatic ecosystem.

References

Berg G.M., Balode M., Purina I., Bekere S., Béchemin C., and Maestrini S.Y. 2003. Plankton community composition in relation to availability and uptake of oxidized and reduced nitrogen. *Aquatic Microbial Ecology*. 30: 263-274.

Berges J.A. Varela D.E., and Harrison P.J. 2002. Effects of temperature on growth rate, cell composition and nitrogen metabolism in the marine diatom *Thalassiosira pseudonana* (Bacillariophyceae). *Marine Ecology Progress Series*. 225: 139-146.

Brandes U.S. 2005. Recapturing the Anacostia River: The Center of 21st Century Washington, DC. *Golden Gate UL Rev.* 35: 411.

Chesapeake Bay Program (CBP). 2002. The State of the Chesapeake Bay: A Report to the Citizens of the Bay Region. Annapolis, MD. Accessed at: http://www.chesapeakebay.net/documents/0659_001.pdf

Cushing D.H. 1989. A difference in structure between ecosystems in strong stratified waters and in those that are only weakly stratified. *Journal of Plankton Research*. 11(1): 1-13.

District of Columbia Water and Sewage Authority. 2002. Combined Sewage System Long Term Control Plan: Final Report. Accessed at: https://www.dcwater.com/sites/default/files/Complete%20LTCP%20For%20CD.pdf

Domingues R.B., Barbosa A.B., Sommer U., and Galvão H.M. 2011. Ammonium, nitrate and phytoplankton interactions in a freshwater tidal estuarine zone: potential effects of cultural eutrophication. *Aquatic Sciences*. 73: 331-343.

Dortch Q. 1990. The interaction between ammonium and nitrate uptake in

   phytoplankton. *Marine Ecology Progress Series*. 61: 183-201.

Dugdale R.C., Wilkerson F.P., Hogue V.E., and Marchi A. 2007. The role of

   ammonium and nitrate in spring bloom development in San Francisco Bay.

   Estuarine, Coastal and Shelf Science. 73: 17-29.

Gao Y., Smith G.J., and Alberte R.S. 2000. Temperature dependence of nitrate

   reductase activity in marine phytoplankton: Biochemical analysis and

   ecological implications. *Journal of Phycology*. 36: 304-313.

Glibert P.M., Wilkerson F.P., Dugdale R.C., Parker A.E., Alexander J., Blaser S., and

   Murasko S., 2014. Phytoplankton communities from San Francisco Bay Delta

   respond differently to oxidized and reduced nitrogen substrates—even under

   conditions that would otherwise suggest nitrogen sufficiency. *Frontiers in*

   Marine Science. 1:17.

Glibert P.M., Wilkerson F.P., Dugdale R.C., Raven J.A., Dupont C.L., Leavitt P.R.,

   Parker A.E., Burkholder J.M., and Kana T.M. 2016. Pluses and minuses of

   ammonium and nitrate uptake and assimilation by phytoplankton and

   implications for productivity and community composition, with emphasis on

   nitrogen-enriched conditions. *Limnology and Oceanography.* 61:165-197.

Goldman J.C. 1993. Potential role of large oceanic diatoms in new primary

   production. *Deep Sea Research Part I: Oceanographic Research Papers*.

   40(1): 159-168.

Jackson, M. 2016. Phytoplankton and nutrient dynamics with a focus on nitrogen

   form in the Anacostia River, in Washington, D.C. and West Lake, in

Hangzhou, China. Masters of Science, University of Maryland, College Park, MD.

Liu D. and Glibert P.M. 2018. Ecophysiological linkage of nitrogen enrichment to heavily silicified diatoms in winter. *Marine Ecology Progress Series*. 604: 51-63.

Lomas M.W., Baer S.E., Acton S., and Krause J.W. 2019. Pumped up by the cold: Elemental quotas and stoichiometry of cold-water diatoms. *Frontiers in Marine Science*. 6: 286.

Lomas M.W. and Glibert P.M. 1999a. Interactions between NH_4^+ and NO_3^- uptake and assimilation: Comparison of diatoms and dinoflagellates at several growth temperatures. *Marine Biology*. 133: 541-551.

Lomas M.W. and Glibert P.M. 1999b. Temperature regulation of nitrate uptake: A novel hypothesis about nitrate uptake and reduction in cool-water diatoms. *Limnology and Oceanography*. 44(3): 556-572.

Lomas M.W. and Glibert P.M. 2000. Comparisons of nitrate uptake, storage, and reduction in marine diatoms and flagellates. *Journal of Phycology*. 36: 903-913.

Parker M.S. and Armbrust E.V. 2005. Synergistic effects of lights, temperature, and nitrogen source on transcription of genes for carbon and nitrogen metabolism in the centric diatom *Thalassiosira pseudonana* (Bacillariophyceae). *Journal of Phycology*. 41(6): 1142-1153.

Patrick R.1948. Factors effecting the distribution of diatoms. *Botanical Review*. 14(8): 473-524.

Probyn T.A. and Painting S.J. 1985. Nitrogen uptake by size-fractionated phytoplankton populations in Antarctic surface waters. *Limnology and Oceanography*. 30(6): 1327-1332.

Shangguan Y., Glibert P.M., Alexander J.A., Madden C.J., and Murasko S. 2017. Phytoplankton assemblage response to changing nutrients in Florida Bay: Results of mesocosm studies. *Journal of Experimental Marine Biology and Ecology*. 494: 38-53.

Solomon, C.M., Jackson M., Glibert P.M., and G. Vazquez. 2019. Chesapeake Bay's 'forgotten' Anacostia River: Eutrophication status and nutrient reduction measures. *Environmental Monitoring and Assessment.* 91: 265.

Song B. and Ward B.B. 2007. Molecular cloning and characterization of high-affinity nitrate transporters in marine phytoplankton. *Journal of Phycology*. 43: 542-552.

Syrett P.J. 1981. Nitrogen metabolism of microalgae. *Canadian Bulletin of Fisheries and Aquatic Sciences*. 210: 182-210.

Chapter 2: Effects of nutrient enrichment on phytoplankton community physiology and composition in the Anacostia River, Chesapeake Bay

Abstract

The Anacostia River is among the smallest, but most polluted tributaries of Chesapeake Bay; however, in recent years, restoration efforts have been implemented to decrease nutrient pollution to this aquatic ecosystem. These restoration efforts may alter the abundance and form of different nutrients in the water column and may ultimately affect the biomass accumulation and community composition of phytoplankton assemblages over time. To determine how changes in the relative abundance of different nutrients alter phytoplankton growth and diversity in the Anacostia River, a mesocosm experiment was conducted in the summer of 2018. The results of this mesocosm study revealed that P-enrichment led to 2-4 times more chl *a* in the mesocosm containers and that N + P enrichments led to higher chl *a* concentrations over time than N or P-alone enrichments. Additionally, diatoms and cryptophytes declined across all nutrient treatments and P enrichment nearly doubled the rate at which diatoms declined. Phosphorus-enrichment significantly increased the abundance of cyanobacteria and decreased the abundance of chlorophytes in the mesocosm containers, leading to changes in the relative abundance of different phytoplankton taxa in those treatments that were P-enriched and those that were not. Together, these results highlight the important role that P-enrichment may play in shaping phytoplankton community composition on the Anacostia River and the synergistic effects that N and P enrichment may have on algal biomass accumulation.

Introduction

Human activities have greatly increased the rate at which nutrients such as nitrogen (N) and phosphorus (P) are supplied to aquatic environments that have led to increases in eutrophication and algal biomass accumulation in marine and freshwater systems around the globe (Nixon 1995, Galloway et al. 2002, Howarth et al. 2011, Glibert et al. 2014a, Glibert et al. 2018). In more recent years, P pollution has declined in many aquatic ecosystems as a result of decreases in human P fertilizer application and increases in the efficiency of P removal from wastewater effluent (Howarth et al. 2011, Glibert et al. 2014a). Conversely, N pollution has remained relatively high and has led to increases in the ambient N:P ratio of many marine and freshwater systems (Glibert et al. 2014a, Bouwman et al. 2017, Glibert 2017, Glibert et al. 2018). In addition to altering the total concentration of N reaching aquatic ecosystems, human activities have also changed the relative abundance of different chemical forms of N in eutrophic waters. An increasing proportion of the N that is supplied to aquatic ecosystems as a result of anthropogenic activities such as fertilizer application and aquaculture is in a reduced form such as ammonium (NH_4^+) or urea, as opposed to an oxidized form such as nitrate (NO_3^-; Glibert et al. 2006, Glibert et al. 2016, Glibert 2017).

It has long been suggested that nutrients will not play a role in shaping phytoplankton community composition as long as nutrients are in saturating concentrations (Reynolds 1999). That is, it has been assumed that if nutrients are not limiting, some other factor must limit phytoplankton growth. More recently, this idea has been challenged (Glibert et al. 2013, Glibert 2017) and field studies have supported the idea that nutrient enrichment may lead to shifts in algal community

composition even when nutrients are readily available in the ambient water column (e.g. Donald et al. 2013, Glibert et al. 2014b, Shangguan et al. 2017b, Swarbrick et al. 2019). For example, increases in the ratio of $NH_4^+ : NO_3^-$ have been associated with shifts in phytoplankton community composition in a number of eutrophic aquatic ecosystems (e.g. Berg et al. 2003, Dugdale et al. 2007, Donald et al. 2011, Glibert et al. 2014).

Ammonium has been described as a "paradoxical" nutrient because its presence has been shown to both stimulate and suppress phytoplankton growth in aquatic ecosystems (Dugdale et al. 2007, 2012, Donald et al. 2013, Glibert et al. 2016, Swarbrick et al. 2019). On the one hand, phytoplankton preferentially use NH_4^+ as an N source because NH_4^+ assimilation is less energetically costly than NO_3^- reduction and assimilation (Harvey 1953, Syrett 1981, Probyn and Painting 1985, Raven et al. 1992). On the other hand, enrichment with NH_4^+ may suppress phytoplankton growth by altering NO_3^- transport and assimilation; however, this effect is more pronounced in some taxa than in others (Dortch 1990, Raven et al. 1992, Glibert et al. 2016 and referenes therein). Reduced rates of productivity in the presence of elevated NH_4^+ conditions have been noted in numerous river, estuarine, and coastal ecosystems impacted by wastewater effluent (MacIsaac et al. 1979, Yoshiyama and Sharp 2006, Dugdale et al. 2007, Waiser et al. 2011, Xu et al. 2012), suggesting that increases in wastewater discharge may repress algal growth and productivity in an aquatic ecosystem.

Previous work has revealed that NH_4^+ suppression of NO_3^- uptake may be more severe for diatoms under some conditions than for other phytoplankton

functional groups such as dinoflagellates, cyanobacteria, and chlorophytes (Lomas and Glibert 1999b, Swarbrick et al. 2019). Diatoms often prefer NO_3^- as an N source (Probyn and Painting 1985, Lomas and Glibert 1999a,b, Domingues et al. 2011) and may thrive under high NO_3^- conditions due to their relatively high NO_3^- uptake rates, their ability to store large amounts of NO_3^-, and their abundance of high-affinity NO_3^- transporters (Lomas and Glibert 2000, Song and Ward 2007, Glibert et al. 2016 and references therein). Diatoms use the reduction of NO_3^- as part of their metabolic strategy to balance cellular energy, especially in cool waters (e.g., Lomas and Glibert 1999a,b), but this pathway may be repressed under conditions of elevated NH_4^+. While diatom growth may be supported by NO_3^- and repressed by NH_4^+, the growth of other phytoplankton taxa, such as non-N_2-fixing cyanobacteria and chlorophytes, often preferentially use reduced forms of N (Dokulil and Teubner 2000, Moore et al. 2002, Berg et al. 2003, Glibert et al. 2004, 2016, Lee et al. 2015, Shangguan et al. 2017a) and do not similarly depend on NO_3^- for cellular energy balance. Therefore, the relative abundance of NH_4^+ and NO_3^- in an aquatic environment may contribute to shifts in phytoplankton community composition depending on the nutritional preferences and physiological capabilities of the phytoplankton taxa that are present when nutrient shifts occur.

The relative availability of P also affects N assimilation, as NO_3^- reduction is an energy-requiring pathway. The nitrate reductase (NR) enzyme catalyzes the first step of NO_3^- reduction and its activity decreases at low phosphate (PO_4^{3-}) concentrations and increases with increases in P (Eppley et al. 1969, Everest et al. 1984). Recently it was shown that the degree of NH_4^+ stimulation or repression by

NH_4^+ was related to the availability of P, not just that of NO_3^- (Swarbrick et al. 2019).
In that study, growth repression by NH_4^+ increased when temperatures and soluble
reactive phosphorus (SRP) concentrations were low and when communities were
dominated by diatoms, cryptophytes, and cyanobacteria (Swarbrick et al. 2019).
Conversely, increases in NH_4^+ promoted phytoplankton growth when waters were
warm, and when soluble reactive phosphorus (SRP) concentrations were high, and
when chlorophytes and non-N_2-fixing cyanobacteria were abundant (Swarbrick et al.
2019).

The Anacostia River, a tributary of Chesapeake Bay, represents an interesting
site to assess the effect of nutrient concentration and form on phytoplankton
community dynamics and N assimilation. The Anacostia River is a eutrophic
freshwater system that has been substantially degraded as a result of chemical and
nutrient pollution over time (Hwang and Foster 2006, McGee et al. 2009, Solomon et
al. 2019). One of the major sources of pollution to the Anacostia River has been the
untreated sewage and stormwater effluent that is discharged into the river from 14
combined sewer overflow outfalls (CSOs) along the water (Brandes 2005, Solomon et
al. 2019). The effluent that enters the river from these point sources is enriched with
NH_4^+ and has helped fuel high biomass algal blooms that have been noted in the
spring and summer months (Jackson 2016, Solomon et al. 2019). Importantly,
restoration efforts in this system are underway that may decrease nutrient pollution
and improve water quality over time. A multi-billion dollar restoration project, the
Anacostia River Tunnel, was implemented in March 2018 to divert CSO effluent to
the Blue Plains Wastewater Treatment Plant (DC Water and Sewer Authority 2017,

Solomon et al. 2019). Following the construction of this tunnel, CSO effluent and nutrient loads reaching the Anacostia River should be reduced, in turn improving water quality and reducing the magnitude of algal blooms in this ecosystem. The concentration of nutrients and the forms of nutrients reaching the river may also change, which could affect the species composition of the phytoplankton blooms that persist in the Anacostia River.

The Anacostia River Tunnel Project will likely alter the concentrations, forms, and ratios of essential nutrients in the water column of this eutrophic river system and may ultimately promote the growth of certain phytoplankton species over others as restoration efforts continue. The implementation of this tunnel is expected to decrease the total concentration of nutrients entering the river, as well as the relative abundance of chemically reduced N species in the water column because CSO effluent is rich is NH_4^+ and urea. Therefore, the overall goal of this study was to conduct a mesocosm manipulation experiment to determine how enrichments with NO_3^-, NH_4^+, urea, PO_4^{3-}, and silicate (Si; a nutrient that is required for diatom growth) in isolation, and in combination, impact phytoplankton nutrient assimilation, biomass, and community composition. Based on previous work conducted in the Anacostia River (Jackson 2016, Solomon et al. 2019), it was hypothesized that increasing the ambient concentration of NO_3^- in the water would increase NO_3^- assimilation and increase the abundance of diatoms, while enrichment with NH_4^+ would decrease NO_3^- assimilation and lead to communities dominated by cyanobacteria and chlorophytes. Phytoplankton communities that were enriched with urea were expected to have shifts in community composition comparable to those noted with NH_4^+ enrichment.

Enrichment with PO_4^{3-} was expected to increase algal NO_3^- assimilation and decrease NH_4^+ growth suppression in the mesocosm containers. Finally, Si enrichments were expected to increase the abundance of diatoms in the mesocosm containers. By measuring a variety of physiological parameters along with concurrent changes in phytoplankton community composition, this mesocosm study provides insight on how nutrient enrichment may stimulate or suppress phytoplankton growth in a nutrient-rich river system.

Materials and Methods

Field methods

Water was collected from Site 1 on the Anacostia River in July 2018 (Fig. 1a). Site 1 was chosen for this study because this site is upstream of the CSOs and may, therefore, reflect how the water will respond to nutrient enrichment downstream. Water temperature, salinity, and dissolved oxygen were recorded using a YSI Pro 2030. Fifteen, 10-liter polyethylene containers were each filled with 5 liters of river water and were transported within 3 hrs to Horn Point Laboratory where nutrient manipulation and analysis took place.

Mesocosm experimental design

The unmanipulated river water was first sampled to characterize the ambient nutrient concentrations and phytoplankton communities, as described below. Then, the containers were dosed with nutrients (Table 1). One of the nutrient treatments was carried out in duplicate (Table 1). The control condition contained only water collected from the river with no added nutrients. In the treatments that were enriched with NO_3^-, NH_4^+, or Si, the concentration of the N or Si enrichment was 20 µM. In

the treatments that were enriched with urea, the concentration of N in the containers was increased by 10 µM-N. In the treatments with added PO_4^{3-}, the enrichment was 1 µM-P. Immediately following nutrient enrichment, Day 1 samples were collected from each experimental container to assess nutrient concentrations, algal physiology, community composition, and productivity, as described below. Containers were then incubated under a single neutral density screen that reduced ambient light intensity by 20% in a flowing, water-filled enclosure. Light intensity and temperature in the incubation pool were measured every 24 hours at the time of daily sample collection.

Analytical protocols

Each morning for 5 days, at 0900, water samples (400 mL) were taken to analyze nutrient concentrations, algal community composition, and NR enzyme activity. These samples were immediately filtered through precombusted (450 °C for 4 hrs) GF/F filters. The filters were retained for enzyme activity assays and for HPLC analysis of microbial community composition, and the filtrate reserved for nutrient analysis. Filters were kept at -80 ºC until analysis. Filtrates were stored at -4 °C. The activity of the NR enzyme was determined according to Eppley et al. (1969) and Berges and Harrison (1995).

Pigment analysis, including chlorophyll (chl) *a*, was undertaken using HPLC, according to Van Heukelem and Thomas (2001, 2005). Fucoxanthin was considered indicative of diatoms, alloxanthin of cryptophytes, zeaxanthin of cyanobacteria, and chl *b* of chlorophytes (Jeffrey and Vesk 1997, Wright et al. 2005). Metagenomic data revealed that dinoflagellates were present at very low abundances in July 2018 when

17

the mesocosm study was conducted and thus diagnostic pigments of dinoflagellates were not considered.

On the collected filtrates, concentrations of NO_3^- were determined using the colorimetric vanadium (III) reduction method (Miranda et al. 2001, Doane and Horwáth 2003), NH_4^+ concentrations were determined according to Holmes et al. (1999), and urea concentrations were analyzed according to Revilla et al. (2005). Silica concentrations were determined at Horn Point Analytical Services Laboratory according to Zimmerman et al. (1977).

Cell abundance was quantified using flow cytometry. Cells were fixed using 10% paraformaldehyde and later analyzed using a BD Accuri C6 flow cytometer with dual excitation (488 nm, 640 nm). Cells were gated by shape and size using forward scatter and side scatter settings. Additionally, four photomultipliers (533/30 nm; green fluorescence, 585/40 nm; phycoerythrin fluorescence, > 670 nm; red fluorescence, 675/25 nm; red fluorescence) were used to detect different phytoplankton functional groups. Cell concentrations were calculated by dividing absolute cell counts by the volume of sample that was analyzed.

A Waltz PHYTO-PAM-II instrument was used to analyze the fluorescence characteristics of the algal communities. Samples for PAM fluorometry were obtained by filtering 200 mL of water onto a GF/F filter and then resuspending the cells in 2 mL of filtrate. Samples were placed in the dark for at least 15 minutes prior to analysis. Algal quantum efficiency (Fv/Fm) was measured for each sample.

Statistical analyses

Changes in algal biomass, physiology, and community composition in each mesocosm container were first characterized by plotting all variables of interest as a function of time. Then, the effects that the different nutrient additions had on algal biomass, physiology, and community composition were evaluated. To determine the effects that nutrient enrichment had on algal biomass, nutrient additions (NO_3^-, NH_4^+, PO_4^{3-}, urea, and Si) were treated as dichotomous, independent variables. Time and nutrient treatment were used as independent predictors in linear mixed effects models to determine the main and interactive effects of nutrient enrichment and time on chl a concentration. In these linear mixed effects models, each experimental container was accounted for as a nested factor within the broader experimental design. The linear mixed effects models were created using R software (R Core Team 2014). To determine the interactive effects of nutrient enrichment and time on algal community composition, the concentrations of the diagnostic pigments were normalized to the concentration of chl a. Then, time and nutrient treatment were used as independent predictors in the linear mixed effects models to determine if the presence or absence of specific nutrients impacted the ratio of the diagnostic pigments relative to chl a throughout the course of the experiment. Similarly, time and nutrient treatment were used as independent predictors in linear mixed effects models to determine how these factors affected enzyme activity and quantum efficiency during the experiment.

The specific effects that P enrichment had on algal biomass, algal community composition, enzyme activity, and quantum efficiency were first evaluated using the linear mixed effects models described above. After creating the linear mixed effects models the data were shuffled and the models were rerun 1,000 times. The

differences between the slopes of the lines with and without P-enrichment in the original linear mixed effects models were compared to the differences in the slopes of the shuffled data to determine whether the diagnostic pigment ratios were significantly altered by P-enrichment over time.

Results

Ambient environmental conditions

Upon sample collection, river water temperature was 26.6 °C, ambient chl *a* concentration was 3.98 µg L^{-1}, and concentrations of NO_3^-, NH_4^+, and urea were 36.82, 5.73, and 1.12 µM-N, respectively (Table 2). All of these values were within 1 standard deviation (SD) of their respective averages for this station and time of year based on previous sampling (Table 2). The DO concentration in the river water was 8.8 mg L^{-1}, which was higher than the average recorded DO value (6.03 ± 1.94 mg L^{-1}), but still fell within two standard deviations of the average (Table 2). The ambient concentrations of PO_4^{3-} and Si in the water were 0.1 µM and 107 µM respectively (Table 2).

Changes over time

Immediately following nutrient enrichment, the average concentrations of NO_3^-, NH_4^+, urea, and Si in the containers that were enriched with these nutrients were 53.94 ± 6.30 µM-N, 26.69 ± 3.08 µM-N, 13.10 ± 2.86 µM-N, and 119.29 ± 5.68 µM-Si, respectively, significantly enriching the concentrations above pre-enrichment levels (Wilcoxon rank-sum test, *p* <0.01; Fig. 2). The concentrations of PO_4^{3-} in the mesocosms over time could not be determined due to analytical error in this analysis. The average concentrations of NO_3^-, NH_4^+, urea, and Si in the containers that were

not enriched with these nutrients were 31.81 ± 6.57 µM-N, 9.03 ± 4.62 µM-N, 0.63 ± 0.33 µM-N, and 103.95 ± 6.55 µM-Si, respectively (Fig. 2).

On day 1 of the experiment, the chl a concentration ranged from 5.25 to 9.37 µg L^{-1} with a mean chl a concentration of 6.97 ± 1.27 µg L^{-1} (Fig. 3). On days 2 and 3 of the mesocosm experiment, chl a concentration ranged from 3.81-14.89 µg L^{-1} and 4.67-32.25 µg L^{-1}, respectively. The most rapid increase in chl a was seen in the NO_3^- + P treatment. By day 4 of the experiment, the concentration of chl a ranged from 5.38 µg L^{-1} in the control container to 42.42 µg L^{-1} in the container that was dosed with NO_3^- and P (Figure 3). In the treatment with P only, chl a declined by day 4. Chlorophyll a did not respond to Si enrichment. In general, the treatment that was replicated (NH_4^+ + P + Si) had similar changes in chl a concentration and community composition between replicates (Table 3). By day 4 of the experiment, the average chl a concentration between the two replicates was 32.75 ± 2.35 µg L^{-1}.

The ratio of fucoxanthin: chl a ratio (indicative of diatoms) declined with time in all of the treatments (Figs. 4a-e). The mean fucoxanthin: chl a ratio on day 1 was 0.041 ± 0.013 while the mean fucoxanthin: chl a ratio on day 4 was 0.011 ± 0.005. In contrast, the ratio of zeaxanthin: chl a (indicative of cyanobacteria) initially declined in all treatments, then increased between days 2 and 3, although the increase was only sustained through day 4 in only those treatments that were enriched with PO_4^{3-} (Figs. 4f-j). As with fucoxanthin: chl a, the alloxanthin: chl a ratio (indicative of cryptophytes) declined with time in all treatments (Figs. 4 k-o). The mean ratio of alloxanthin: chl a ratio was 0.063 ± 0.007 on day 1 and declined to 0.018 ± 0.011 by day 4. The highest chl b: chl a ratio (indicative of chlorophytes) was 0.16 and was

noted in the control treatment on day 4 (Figs. 4p-t) and the lowest chl b: chl a ratio was 0.056 and was noted in the P-enriched treatment on day 4 (Fig. 4s).

The rate of NR activity significantly declined with time (Linear model, $p <$ 0.01; $n = 56$, Figs. 5a-e). The average activity of NR on day 1 was 4.25 ± 2.52 pmol NO_2^- formed hr^{-1} cell^{-1} and on day 4 was 0.057 ± 0.064 pmol NO_2^- formed hr^{-1} cell^{-1}. There was a spike in NR activity on day 2 of the experiment in the treatments that were enriched with N + P + Si (Fig. 5a-c). This spike in NR activity was more prominent in the treatments that were enriched with NO_3^- + P + Si and urea + P + Si than in the treatment that was enriched with NH_4^+ + P + Si (Fig. 5a-c).

The initial total community Fv/Fm reflected that of actively photosynthesizing cells, with a value of 0.5 (Fig. 6). Values remained high throughout the time course for the treatments with NO_3^- and NO_3^- + Si. Curiously, some of the treatments with + Si showed an initial decline in Fv/Fm, with values of < 0.2 for the +Si treatment alone, but recovery was seen by day 2. Fv/Fm declined in the treatments with NH_4^++P +Si and a steady decline was also seen in the urea treatment and in the urea + P + Si treatment. The control treatment showed a decline on day 3 but recovery by day 4.

Changes with substrate

In all of the treatments that were enriched with P, the concentration of chl a and the total cell abundance increased significantly over time (Linear mixed effects model, $p < 0.01$, $n = 56$; Fig. 7). Conversely, when considered collectively, additions of NO_3^-, urea, or Si without P did not significantly alter the chl a concentration, although cell abundance did increase. The average concentration of chl a with added P was 31.99 ± 6.49 µg L^{-1} on day 4, while the average concentration of chl a in the

containers that were not P-enriched was 6.99 ± 2.38 µg L^{-1} on day 4. Enrichment with

NO_3^-, NH_4^+, or urea also affected the concentration of chl a in the mesocosms that

were P-enriched. The day 4 concentration of chl a in the container that was enriched

with P alone was 21.92 µg L^{-1}, while the average chl a concentration in the

mesocosms that were enriched with P and N was 33.43 ± 5.47 µg L^{-1} on day 4.

There were also some significant differences in algal community composition

in P-enriched treatments. While, as previously noted, the fucoxanthin: chl a ratio

declined with time in all of the mesocosm treatments (Figs. 4a-e), enrichment with P

significantly and negatively affected this ratio over time (Linear mixed effects model,

$p < 0.05$, $n = 56$, Fig. 8a). Conversely, enrichment with P significantly increased the

ratio zeaxanthin: chl a over time (Linear mixed effects model, $p < 0.01$, $n = 56$, Fig.

8b). The ratio of alloxanthin: chl a declined with time across all nutrient enrichments

but this general decline in alloxanthin concentration was not significantly affected by

P-enrichment ($p = 0.36$, n $= 56$, Figs. 4k-o, 8c). There was a significant difference in

the ratio of chl b: chl a over time in the treatments that were enriched with P

compared to those that were not (Linear mixed effects model, $p < 0.01$, $n = 56$, Fig.

8d). On day 4 of the experiment, the treatments that were enriched with P had a

significantly lower chl b: chl a ratio than the treatments that did not contain added P

(Wilcoxon rank sum test, $p < 0.01$, $n = 56$, Fig. 8d).

Differences were also noted in algal biomass and enzyme activity with

changes in N concentration. Algal biomass increased significantly as the

concentrations of NO_3^- and urea declined in the P-enriched mesocosm containers

(Linear mixed effects models, $p < 0.01$, $n = 56$, Fig. 9a and $p < 0.05$, $n = 56$, Fig. 9g

for NO_3^- and urea respectively). Similar drawdowns of NH_4^+ were noted as chl *a*
increased in the P-enriched mesocosms, though these results were not statistically
significant (Linear mixed effects models, $p = 0.11$, $n = 56$, Fig. 9d). The activity of
NR increased when NO_3^- concentrations were high in the P-enriched containers and
remained relatively stable when P was not supplied to the mesocosms, though this
relationship was not statically significant (Linear mixed effects model, $p = 0.069$, $n = 56$, Fig. 9b). Additions of P did not significantly affect the relationship between N
concentration and algal Fv/Fm for any of the different N forms (Fig. 9c, f, i).

Discussion

The overarching goal of this study was to investigate the effects of nutrient
enrichment on algal physiology and community composition in a eutrophic
freshwater ecosystem. The effects were considered to be representative of the types of
effects that might be seen along the Anacostia River receiving outflow from sewage
and CSOs. The largest response in biomass was in treatments with an enrichment of
P, and no effect was seen in the treatments with an enrichment of Si alone. Moreover,
the combination of N plus P led to the highest biomass accumulation; the treatment
with P only became limited by N by day 3, and thus the combination of nutrients
promoted highest biomass accumulation. Addition of Si yielded no biomass changes,
although in all the treatments with Si there was an unexplained initial drop in
quantum efficiency. The higher biomass accumulation in the treatments with N and P
is consistent with the findings of Zohary et al. (2005), North et al. (2007), Xu et al.
(2014), Müller and Mitrovic (2015), and Paerl et al. (2015) who have interpreted such
an effect to be co-limitation.

The results obtained from this study did not reveal significant changes in algal biomass or community composition as a result of enrichment with different N forms. This finding does not agree with the results of a 3-year Anacostia River monitoring study conducted by Solomon et al. (2019). In the Solomon et al. (2019) study the fucoxanthin: chl a ratio increased as NO_3^- concentrations in the river increased, while the zeaxanthin: chl a ratio in the river increased as NH_4^+ concentrations increased. It is possible that at other times throughout the year or under a different suite of environmental conditions, the effects of N form on algal biomass and community composition may be observed under NO_3^- or NH_4^+-enriched conditions.

Although differences in N form alone did not lead to notable in changes in algal biomass and community composition in this study, the significant role that P-enrichment played in shaping the mesocosm phytoplankton communities may be explained when considering the effects that P-enrichment can have on NH_4^+ growth suppression. Swarbrick et al. (2019), analyzing 16 years of bioassays with NH_4^+ enrichment in a freshwater lake in Canada, showed that NH_4^+ can differentially stimulate or suppress algal growth depending on ambient algal community composition, water temperature, and SRP concentration at the time of NH_4^+ enrichment. Specifically, the results of the Swarbrick et al. (2019) study found that algal growth stimulation by NH_4^+ increased with increasing temperature under high-P conditions. Similarly, in the same P-rich lake system, Donald et al. (2013) showed that NH_4^+-enrichment led to significant increases in cyanobacterial abundance and significant decreases in diatom abundance. The results obtained from this Anacostia River mesocosm study agree in part with the findings outlined by Donald et al. (2013)

and Swarbrick et al. (2019), in that P was an important predictor in determining how algal communities would respond to high ambient and enriched NH_4^+ conditions (Fig. 8). Although temperature was not a variable that was manipulated in this study, water temperatures were consistently warm and were comparable to the warmer water temperature trials noted in the Swarbrick et al. (2019) study, suggesting that warmer water temperatures along with P availability may be important environmental factors influencing NH_4^+ growth stimulation in cyanobacteria. It is known that cyanobacteria are favored under warm conditions (e.g. Paerl et al. 1985, Paul 2008, Carey et al. 2012), while diatoms are favored under cooler conditions (Probyn and Painting 1985, Lomas and Glibert 1999b). The results of this study build on studies by Swarbrick et al. (2019) and Donald et al. (2013) by suggesting that NH_4^+ growth stimulation of cyanobacteria may occur at the same time as NH_4^+ growth suppression of diatoms and that both of these processes may be directly related to P availability (Figs. 8a, b).

The important role that P-enrichment may play in altering algal NH_4^+ growth suppression may not always be straightforward. In a mesocosm manipulation experiment carried out by Shangguan et al. (2017b) in Florida Bay, NO_3^- + P additions initially promoted the growth of diatoms and then led to declines in diatom abundance and increases in cyanobacterial abundance. Unlike the Shangguan et al. (2017b) study, notable increases in diatom abundance were not observed at any time point during this experiment (Figs. 4a-e, 8a). The lack of a diatom response noted in this study may be due to the fact that the P-enrichments made in this study were lower than those made in the single enrichments of the Shannguan et al. (2017) study, suggesting that diatom growth may be supported when P concentrations are higher or

when N:P ratios are lower. Different diatom species may also have been present in the ambient communities of these different studies. Despite the differences noted between this study and the Shannguan et al. (2017b) study, both of these experiments support the idea that cyanobacteria may thrive in an aquatic ecosystem that has a relatively high concentration of NH_4^+ and a relatively low concentration of P.

Cyanobacteria may outcompete other algal taxa under high-N and low-P conditions because cyanobacteria are good competitors for inorganic P, can use organic P forms, and can use non-P lipids under P-limited conditions (Glibert et al. 2004, Van Mooey et al. 2009, O'Neil et al. 2012). In addition to the similar cyanobacterial response noted in this study and the Shannguan et al. (2017b) study, both of these studies also demonstrated that N and P enrichment together led to higher algal biomass accumulation in the experimental containers than adding either nutrient alone, regardless of which N form (NO_3^-, NH_4^+, or dissolved organic N/urea) was supplied to the algae. Therefore, the results of this study and the Shangguan et al. (2017b) study add to the growing body of knowledge that suggests that N and P pollution must both be controlled to effectively manage eutrophication in aquatic ecosystems (Paerl et al. 2004, Conley et al. 2009, Paerl et al. 2011, Chen et al. 2012).

The dual effect of N and P on biomass accumulation has previously been interpreted as co-limitation by both nutrients (e.g., Zohary et al. 2005, North et al. 2007, Xu et al. 2014, Müller and Mitrovic 2015, Paerl et al. 2015). Yet, it can also be interpreted as sequential nutrient limitation. In this study, the P-only treatment showed evidence of biomass decline by day 4 (Fig. 3d), but no such decline was noted with added N + P. Moreover, Fv/Fm declined from day 2 to 4 in the P only

treatment, suggesting that the algae growing in this mesocosm container may have been stressed as a result of N limitation. The daily sample collection that was undertaken in this study allowed the effects of sequential nutrient limitation to be distinguished from the effects of nutrient co-limitation, as single and point measurements may be falsely interpreted as nutrient co-limitation.

In addition to the notable effects that N+P-enrichment had on algal biomass and phytoplankton community dynamics in this study, differences in algal nutrient use were also documented throughout the course of the study. The nutrient concentration data revealed that NH_4^+ drawdown between days 1 and 2 of the experiment occurred faster than NO_3^- drawdown in the P-enriched mesocosm containers, suggesting that NH_4^+ may have been the preferred N source for the phytoplankton that were growing in the P-enriched waters (Figure 2). This preference for NH_4^+ over NO_3^- by cyanobacteria has been well-documented in other systems (Berg et al. 2003, Ferber et al. 2004, Glibert et al. 2006, 2014b, Donald et al. 2011, Paerl et al. 2011, Shangguan et al. 2017b), as well as in the Anacostia River (Jackson 2016, Solomon et al. 2019). Although NH_4^+ drawdown between days 1 and 2 by the P-enriched mesocosm phytoplankton communities was greater than that of NO_3^-, by day 4 of the experiment, NO_3^- concentrations in the P-enriched mesocosms were substantially reduced (Fig. 2), demonstrating that the phytoplankton in the P-enriched containers were using the NO_3^- along with the NH_4^+ that was available in the water. Additionally, the activity of the activity of the NR enzyme tended to increase under high-NO_3^- and P-enriched conditions (Fig. 9b), suggesting that NO_3^- reduction and assimilation may have occurred when these nutrients were readily available to the P-

enriched mesocosm phytoplankton communities. Lastly, algal Fv/Fm tended to decrease as N was depleted in the P-enriched mesocosm containers (Fig. 9c,f,i), suggesting that the phytoplankton in the P-enriched waters became N-limited over time and that the P-enriched communities were using all forms of N to some extent throughout the course of the experiment. These nutrient and physiological data support the notion that NO_3^- assimilation may be dependent on P availability in an aquatic ecosystem and that low P availability may prevent phytoplankton from accessing all of the N available in the DIN pool.

Conclusion

The results obtained from this study highlight the important role that both N and P concentrations may play in altering algal biomass and community composition in a eutrophic freshwater system, even when nutrient concentrations in the ambient water column are already at or near saturating levels. Additionally, the results of this study suggest that NH_4^+ may be the preferred N source for the cyanobacteria that are growing in the Anacostia River during the summer months and that P-availability may play a role in NH_4^+ growth stimulation and suppression of various phytoplankton taxa present in the water column. As efforts to restore water quality in the Anacostia River continue, the dual control of both N and P pollution must be considered in order to ensure environmental conditions do not promote the growth of high biomass and potentially harmful algal blooms. The implementation of the Anacostia River Tunnel will likely decrease the amount of nutrient pollution that reaches the river waters and may potentially lead to reductions in eutrophication over time.

Table 1. The experimental treatments that were used in this study.

Treatment	Replicates
Control	1
+ 20 μM NO_3^-	1
+ 10 μM Urea	1
+ 1 μM PO_4^-	1
+ 20 μM Si	1
+ 20 μM NO_3^- + 1 μM PO_4^-	1
+ 20 μM NH_4^+ + 1 μM PO_4^-	1
+ 10 μM Urea + 1 μM PO_4^-	1
+ 20 μM NO_3^- + 20 μM Si	1
+ 10 μM Urea + 20 μM Si	1
+ 20 μM NO_3^- + 1 μM PO_4^- + 20μM Si	1
+ 20 μM NH_4^+ + 1 μM PO_4^- + 20μM Si	2
+ 10 μM Urea + 1 μM PO_4^- + 20μM Si	1

Table 2: Ambient environmental conditions at Site 1 on the Anacostia River, Chesapeake Bay on the day that the mesocosm study began.

Parameter	Ambient measurement	Average July measurement at Site 1 2013-2018 (mean ± sd)
Temperature (°C)	26.6	25.6 ± 2.0
Dissolved oxygen (mg L^{-1})	8.8	6.03 ± 1.94
NO$_3^-$ (µM)	36.82	39.8 ± 14.4
NH$_4^+$ (µM)	5.73	6.88 ± 5.25
Urea (µM)	1.12	1.17 ± 1.16
PO$_4^{3-}$ (µM)	0.1	NA
Si (µM)	107	NA
Chlorophyll *a* (µg L^{-1})	3.98	11.93 ± 9.14
Zeaxanthin (µg L^{-1})	0.54	0.161 ± 0.065
Alloxanthin (µg L^{-1})	0.21	0.417 ± 0.185
Fucoxanthin (µg L^{-1})	0.27	0.636 ± 0.221
Chlorophyll *b* (µg L^{-1})	0.51	0.909 ± 0.203
Zeaxanthin/Chlorophyll *a*	0.14	0.029 ± 0.013
Alloxanthin/Chlorophyll *a*	0.053	0.071 ± 0.029
Fucoxanthin/ Chlorophyll *a*	0.068	0.107± 0.019
Chlorophyll *b*/ Chlorophyll *a*	0.13	0.156 ± 0.030

Table 3: Chlorophyll *a* concentrations and pigment ratios in the mesocosm containers that were replicated (NH_4^+ + P +Si) and the mean and standard deviation of these measurements between the two replicates.

Parameter	Day	NH_4^+ + P + Si #1	NH_4^+ + P + Si #2	Mean ± Standard Deviation
Chlorophyll *a* (μg L^{-1})	1	6.72	6.55	6.64 ± 0.12
Fucoxanthin: Chlorophyll *a*	1	0.042	0.031	0.036 ± 0.0077
Zeaxanthin: Chlorophyll *a*	1	0.094	0.102	0.098 ± 0.006
Alloxanthin: Chlorophyll *a*	1	0.057	0.073	0.065 ± 0.011
Chlorophyll *b*: Chlorophyll *a*	1	0.097	0.094	0.095 ± 0.002
Chlorophyll *a* (μg L^{-1})	2	10.65	10.50	10.58 ± 0.11
Fucoxanthin: Chlorophyll *a*	2	0.013	0.012	0.013 ± 0.0009
Zeaxanthin: Chlorophyll *a*	2	0.064	0.062	0.063 ± 0.0013
Alloxanthin: Chlorophyll *a*	2	0.026	0.028	0.026 ± 0.0037
Chlorophyll *b*: Chlorophyll *a*	2	0.13	0.11	0.12 ± 0.0091
Chlorophyll *a* (μg L^{-1})	3	26.44	28.16	27.30 ± 1.21
Fucoxanthin: Chlorophyll *a*	3	0.006	0.009	0.008 ± 0.002
Zeaxanthin: Chlorophyll *a*	3	0.151	0.151	0.151 ± 9.1 e-6
Alloxanthin: Chlorophyll *a*	3	0.010	0.013	0.011 ± 0.002
Chlorophyll *b*: Chlorophyll *a*	3	0.081	0.066	0.074 ± 0.01
Chlorophyll *a* (μg L^{-1})	4	34.41	31.08	32.75 ± 2.35
Fucoxanthin: Chlorophyll *a*	4	0.005	0.005	0.005 ± 0.0004
Zeaxanthin: Chlorophyll *a*	4	0.14	0.21	0.17 ± 0.05
Alloxanthin: Chlorophyll *a*	4	0.010	0.009	0.010 ± 0.0008
Chlorophyll *b*: Chlorophyll *a*	4	0.084	0.076	0.080 ± 0.006
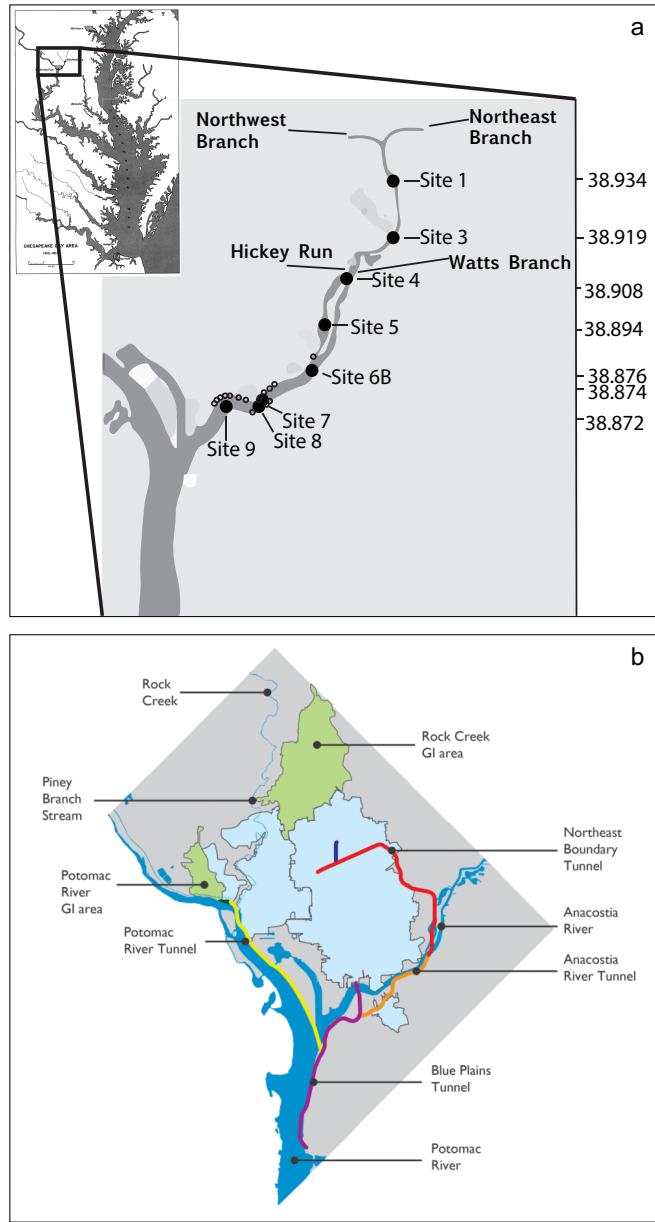
Figure 1. Map of the Anacostia River, Chesapeake Bay monitoring sites (a) and map of the Anacostia River Tunnel Project (b). The small open circles in panel a indicate the sites of combined sewer overflow outfalls. The mesocosm study was conducted at Site 1 above the outfall sites. The monitoring map was reproduced from Solomon et al. (2019) with permission of Springer and the tunnel project map was obtained from D.C. Water and Sewer Authority (2017).
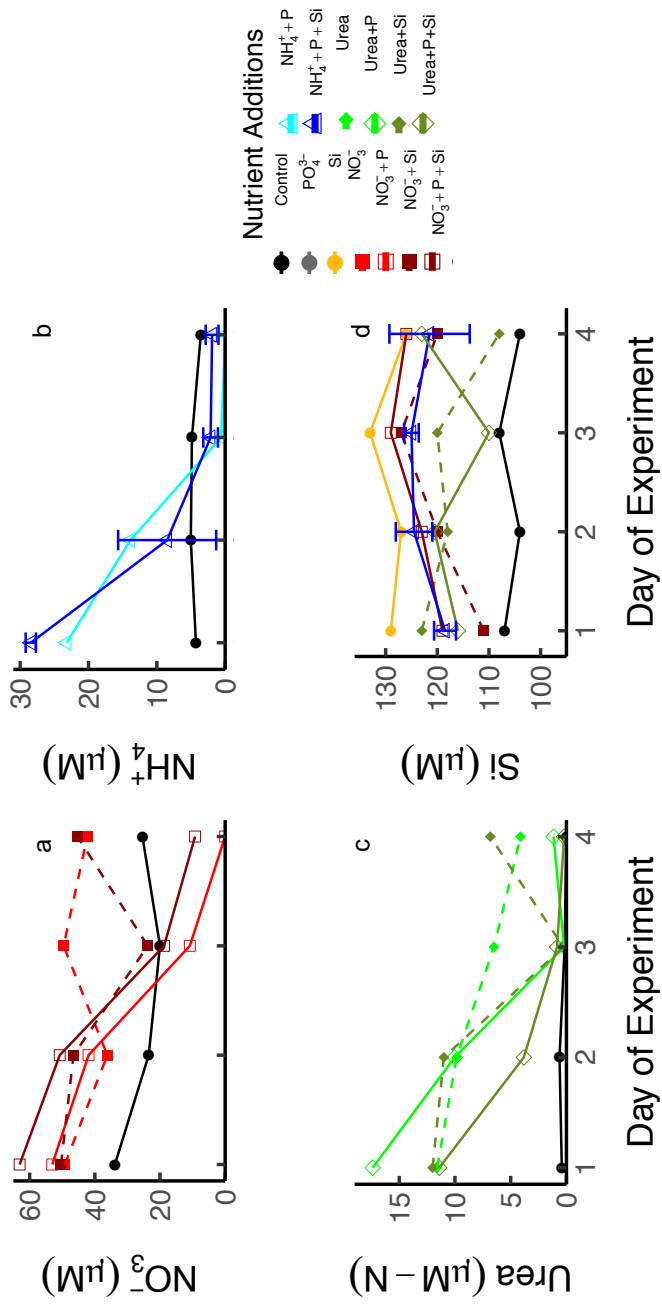
Figure 2: Change in the concentrations of NO_3^- (a), NH_4^+ (b), Urea (c), and and Si (d) measured in the mesocosm containers over time.
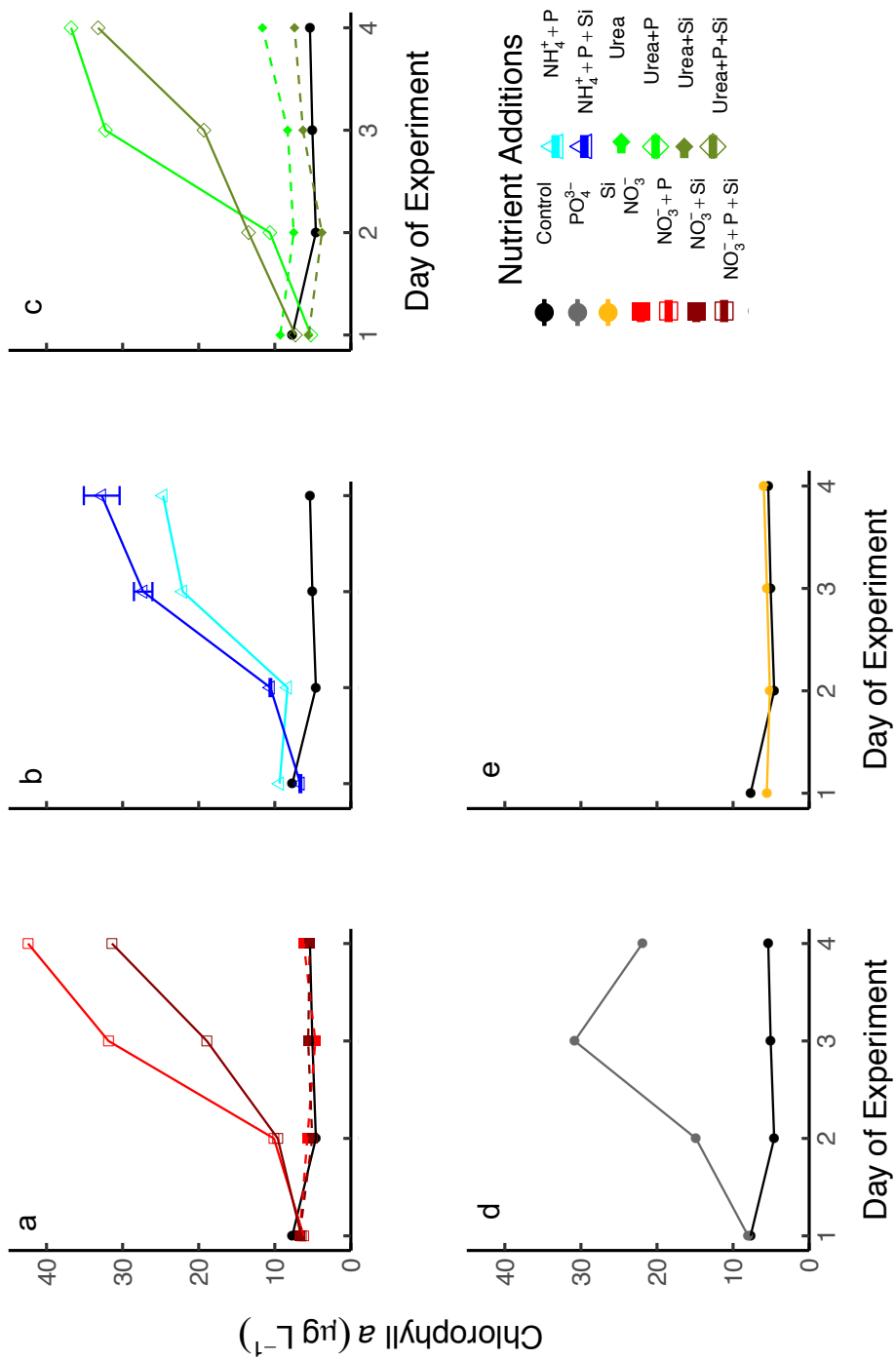
Figure 3: Change in the concentration (μg L^{-1}) of chlorophyll *a* over time. Panels a, b, and c show all treatments that were enriched with NO$_3^-$, NH$_4^+$ and urea respectively. Panel d shows the treatment that was enriched with PO$_4^{3-}$ alone and panel e shows the treatment that was enriched with Si alone. The control treatment was reproduced in each panel for reference.
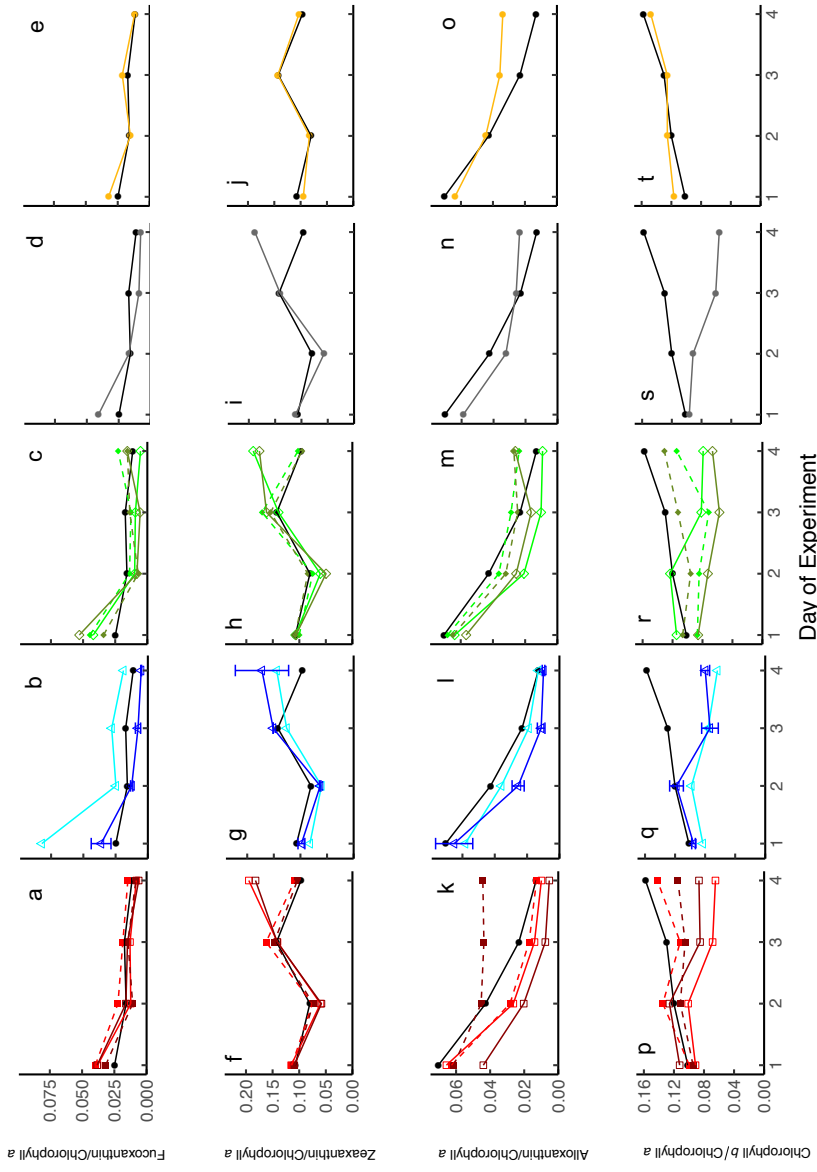
Figure 4: The ratio of fucoxanthin (panels a-e), zeaxanthin (panels f-j), alloxanthin (panels k-o), and chlorophyll b (chl b; panels p-t) to chlorophyll a (chl a) over time. Panels a, f, k, and p show all NO_3^- treatments, panels b, g, l, and q show all NH_4^+ treatments, panels c, h, m, and r show all urea treatments, panels d, i, n, and s show the PO_4^{3-} treatment, and panels e, j, o, and t show the Si treatment. Data for the control treatment were reproduced for reference in each panel. The ratio of fucoxanthin to chl a is indicative of diatoms, the ratio of zeaxanthin to chl a is indicative of cyanobacteria, the ratio of alloxanthin to chl a is indicative of cryptophytes, and the ratio of chl b to chl a is indicative of chlorophytes. Legend as in Figure 2.

36
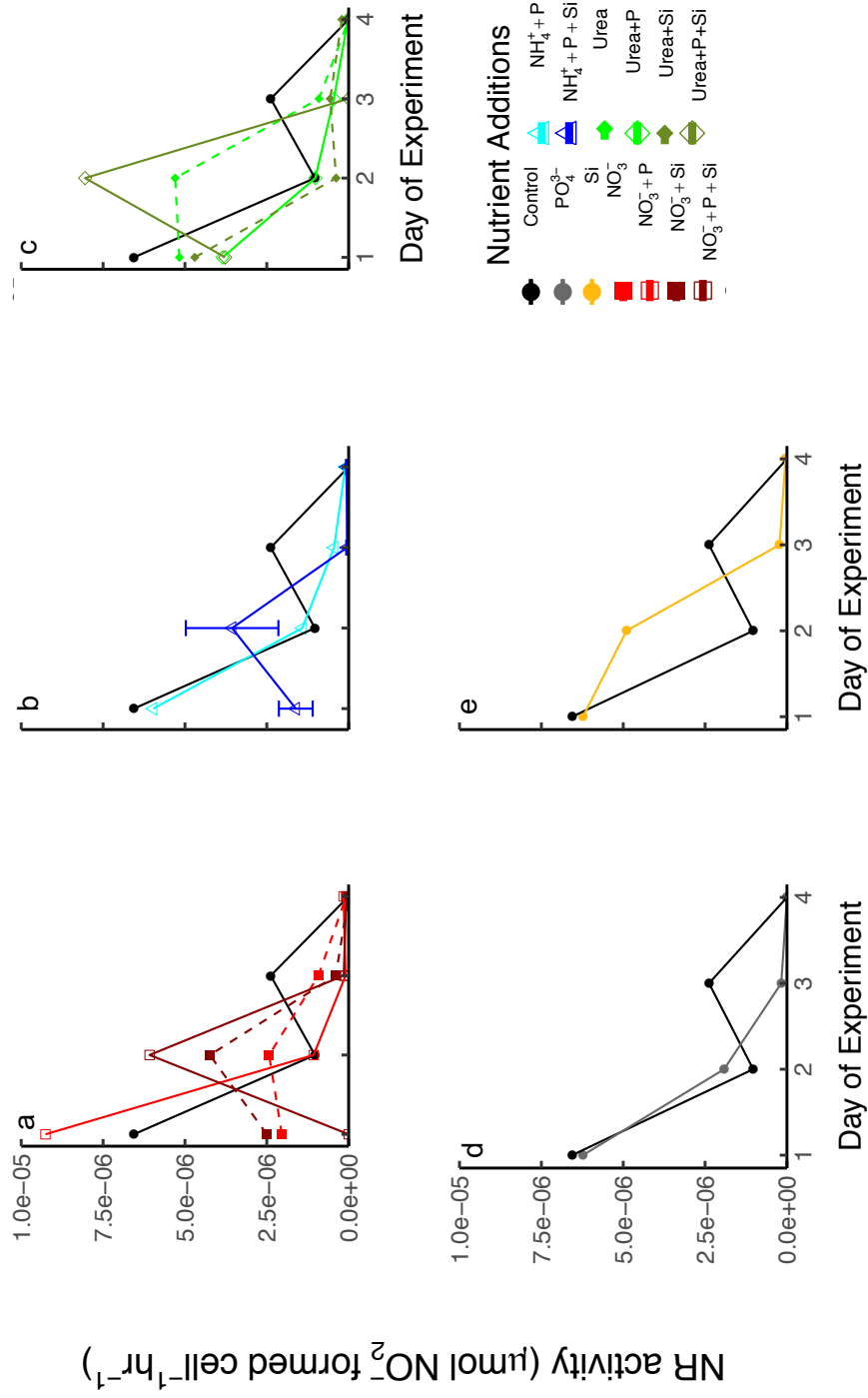
Figure 5: Activity of the NR enzyme over time. Panel a shows all of the NO_3^- treatments, panel b shows all of the NH_4^+ treatments, panel c shows all of the urea treatments, panel d shows the PO_4^{3-} treatment, and panel e shows the Si treatment. The control treatment data were reproduced in each panel for reference.
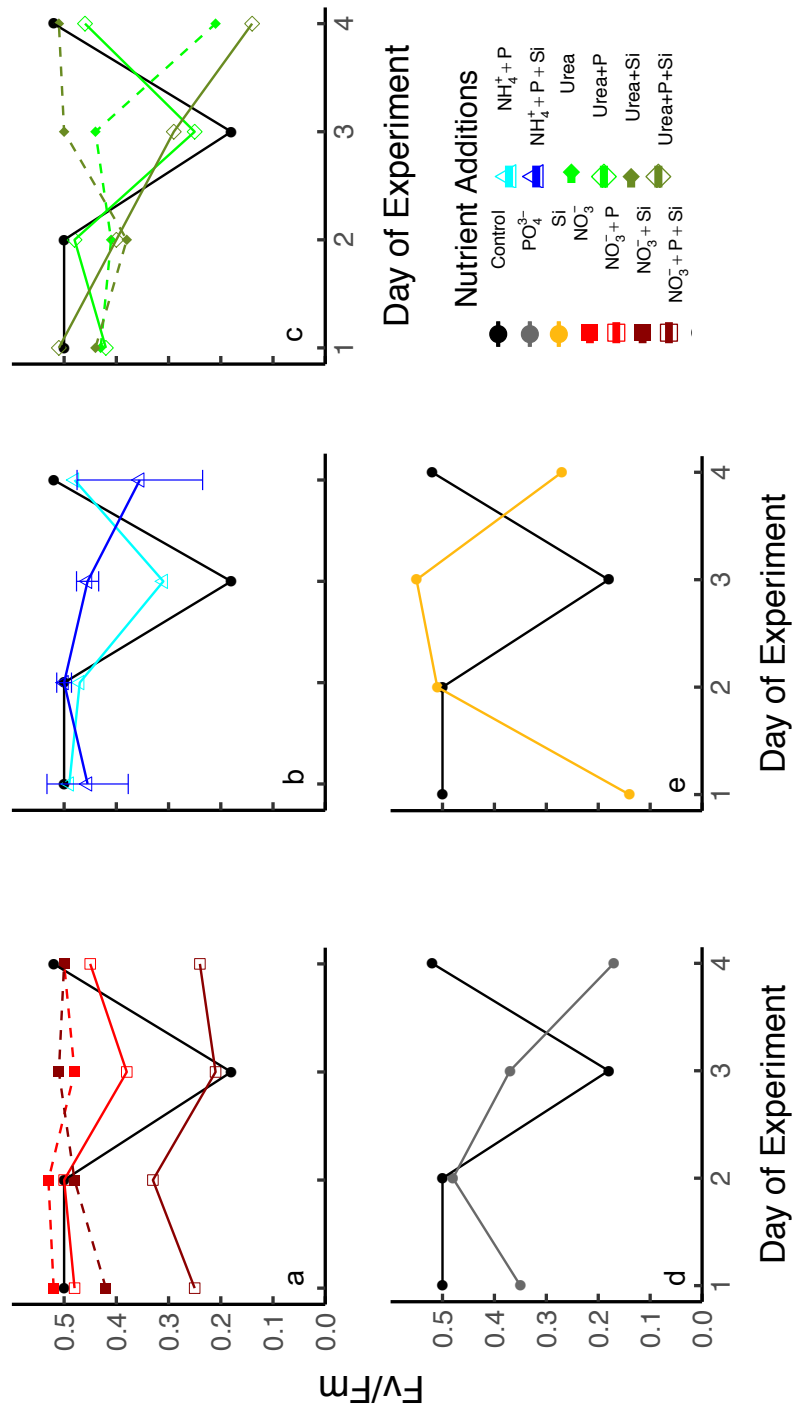
Figure 6: Algal quantum efficiency (Fv/Fm) in the different mesocosm treatments over time. Panel a shows all of the NO_3^- treatments, panel b shows all of the NH_4^+ treatments, panel c shows all of the urea treatments, panel d shows the PO_4^{3-} treatment, and panel e shows the Si treatment. The control treatment data were reproduced in each panel for reference.
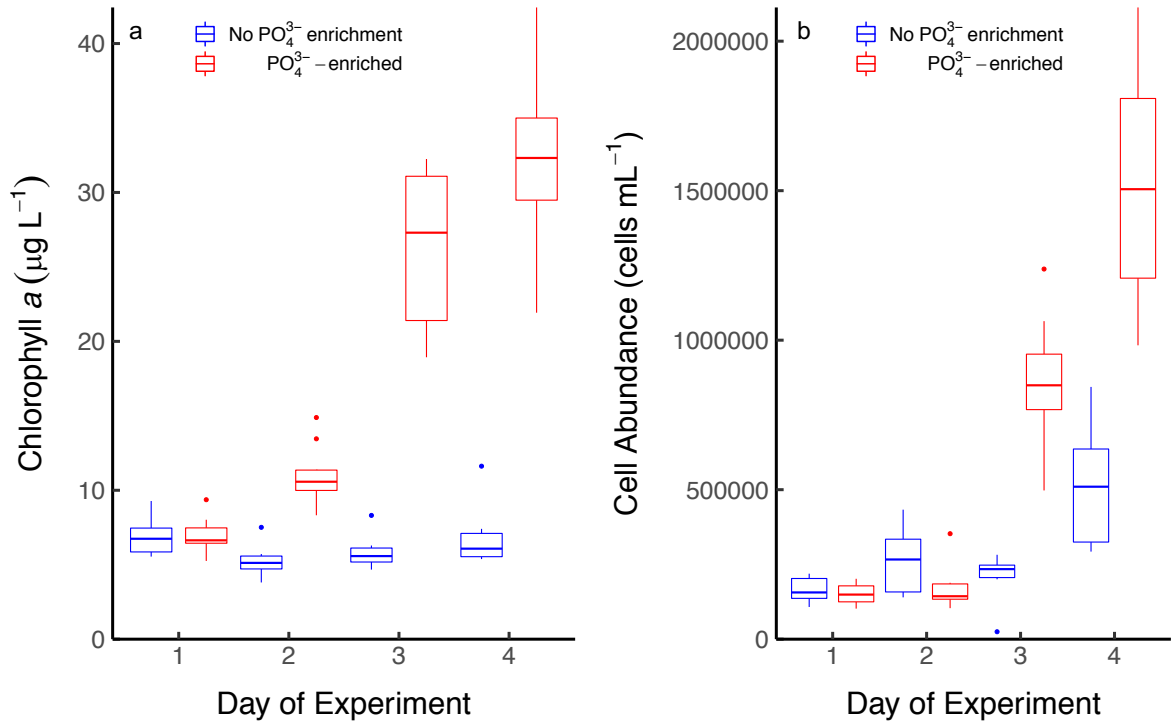
Figure 7: Concentration of chlorophyll *a* (a) and total cell abundance (b) as a function of time for all treatments that were enriched with PO_4^{3-} and those that were not.
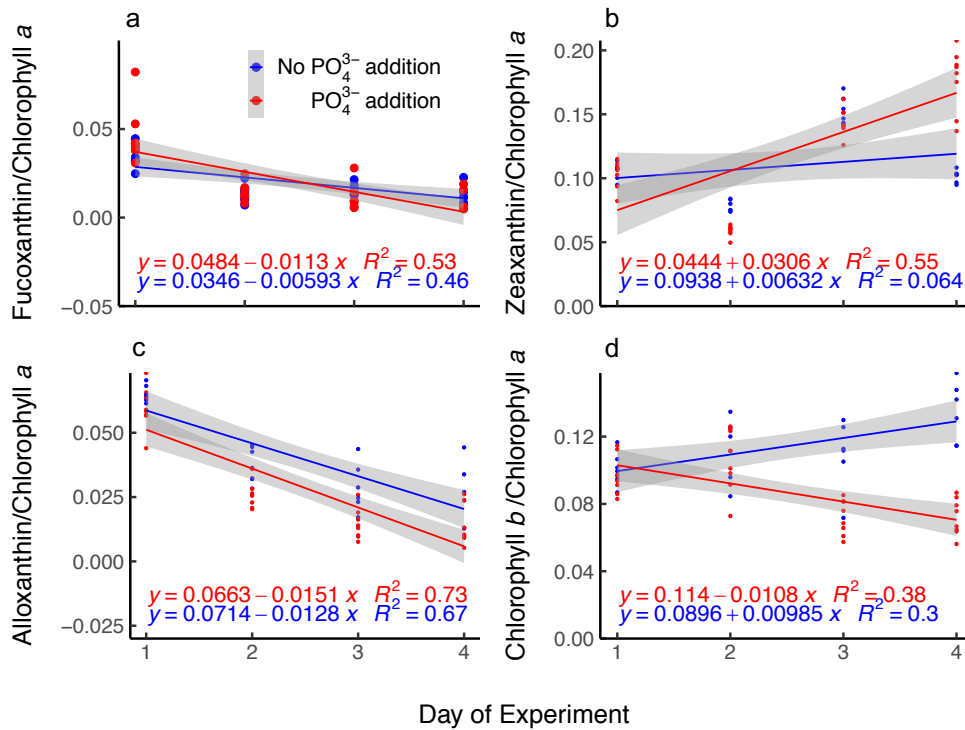
Figure 8: The ratio of the fucoxanthin (a), zeaxanthin (b), alloxanthin (c), and chlorophyll b (chl b, d) to chlorophyll a (chl a) over time differentiated by those treatments that were enriched with PO_4^{3-} and those that were not. Fucoxanthin is indicative of diatoms, zeaxanthin is indicative of cyanobacteria, alloxanthin is indicative of cryptophytes, and chl b is indicative of chlorophytes.
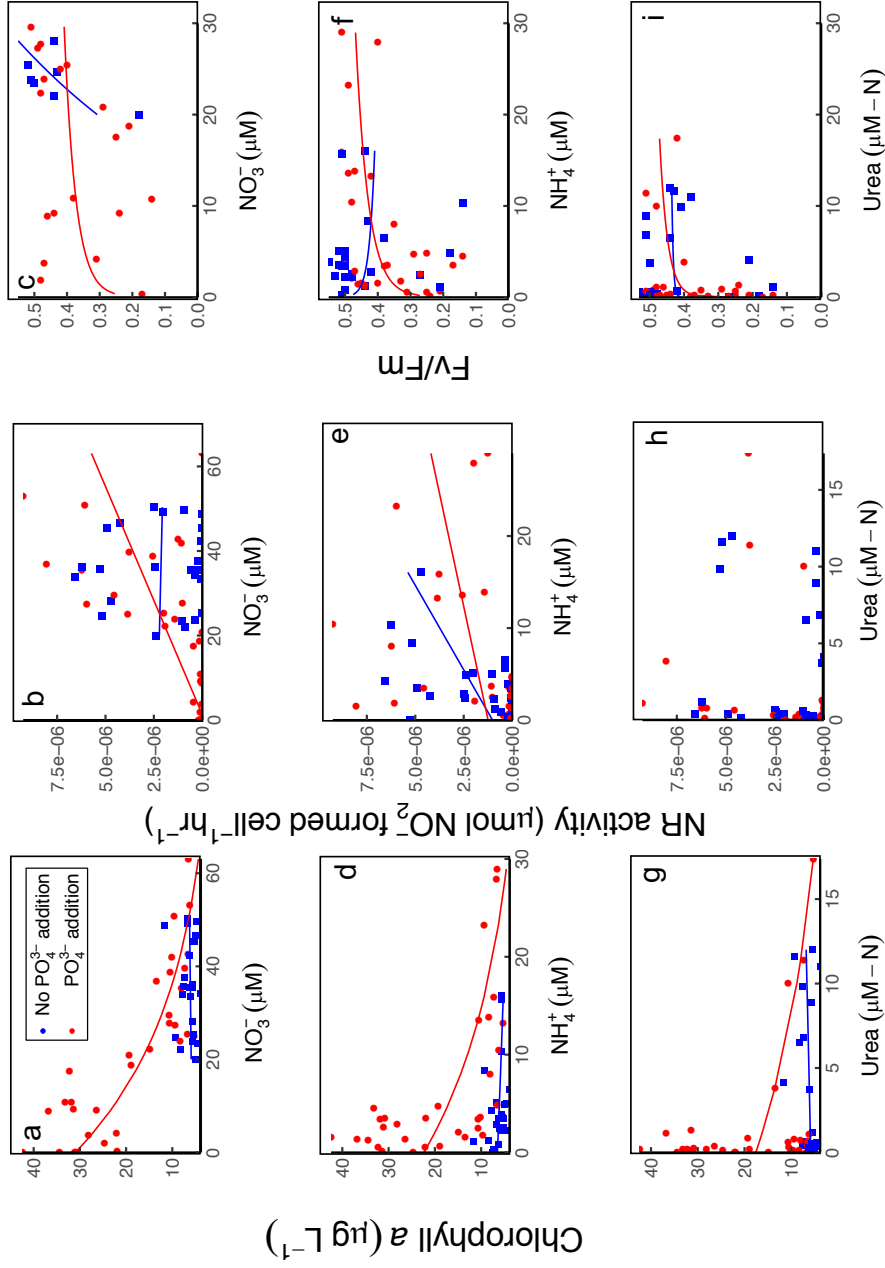
Figure 9: Chlorophyll *a*, NR activity, and total community Fv/Fm as a function of NO_3^- concentration (panels a-c), NH_4^+ concentration (panels d-f), and urea concentration (panels g-i) in the mesocosm containers that were PO_4^{3-}-enriched and in those that did not contain added PO_4^{3-}.

41

References

Berg G.M., Balode M., Purina I., Bekere S., Béchemin C., and Maestrini S.Y. 2003. Plankton community composition in relation to availability and uptake of oxidized and reduced nitrogen. *Aquatic Microbial Ecology*. 30: 263-274.

Berges J.A. and Harrison P.J. 1995. Nitrate reductase activity quantitatively predicts the rate of nitrate incorporation under steady state light limitation: A revised assay and characterization of the enzyme in three species of marine phytoplankton. *Limnology & Oceanography*. 40(1): 82-93.

Bouwman A.F., Beusen A.H.W., Lassaletta L., van Apeldoorn D.F., van Grinsven H.J.M, Zhang J., and van Ittersum M.K. 2017. Lessons from temporal and spatial patterns in global use of N and P fertilizer on cropland. *Scientific Reports.* 7: 40366.

Brandes U.S. 2005. Recapturing the Anacostia River: The Center of 21st Century Washington, DC. *Golden Gate UL Rev.* 35: 411.

Carey C.C., Ibelings B.W., Hoffman E.P., Hamilton D.P., and Brookes J.D. 2012. Eco-physiological adaptations that favour freshwater cyanobacteria in a changing climate. *Water Research*. 46: 1394-1407.

Chen N., Peng B., Hong H., Turyaheebwa N., Cui S., and Mo X. 2012. Nutrient enrichment and N:P ratio decline in a costal bay—river system in southeast China: The need for a dual nutrient (N and P) management strategy. *Ocean & Coastal Management*. 32(4): 593-601.

Conley D.J., Paerl H.W., Howarth R.W., Boesch D.F., Seitzinger S.P., Havens K.E., Lancelot C., and Likens G.E. 2009. Controlling eutrophication: nitrogen and phosphorus. *Science*. 323: 1014-1015.

District of Columbia Water and Sewer Authority. 2017. Clean water projects. Accessed at: https://www.dcwater. com/projects.

Doane T.A. and Horwáth W.R. 2003. Spectrophotometric determination of nitrate with a single reagent. *Analytical Letters*. 36(12): 2713-2722.

Dokulil M.T. and Teubner K. 2000. Cyanobacterial dominance in lakes. *Hydrobiologia*. 438: 1-12.

Domingues R.B., Barbosa A.B., Sommer U., and Galvão H.M. 2011. Ammonium, nitrate and phytoplankton interactions in a freshwater tidal estuarine zone: potential effects of cultural eutrophication. *Aquatic Sciences*. 73: 331-343.

Donald D.B., Bogard M.J., Finlay K., and Leavitt P.R. 2011. Comparative effects of urea, ammonium, and nitrate on phytoplankton abundance, community composition, and toxicity in hypereutrophic freshwaters. *Limnology and Oceanography*. 56(6): 2161-2175.

Donald D.B., Bogard M.J., Finlay K., Bunting L., and Leavitt P.R. 2013. Phytoplankton-specific response to enrichment of phosphorus-rich surface waters with ammonium, nitrate, and urea. *PLOS One*. 8(1): e53277.

Dortch Q. 1990. The interaction between ammonium and nitrate uptake in phytoplankton. *Marine Ecology Progress Series*. 61: 183-201.

Dugdale R.C., Wilkerson F.P., Hogue V.E., and Marchi A. 2007. The role of
    ammonium and nitrate in spring bloom development in San Francisco Bay.
    Estuarine, Coastal and Shelf Science. 73: 17-29.

Dugdale R., Wilkerson F., Parker A.E., Marchi A., and Taberski K. 2012. River flow
    and ammonium discharge determine spring phytoplankton blooms in an
    urbanized estuary. *Estuarine, Coastal and Shelf Science*. 115: 187-199.

Eppley R.W., Coatsworth J.L., and Solórzano L. 1969. Studies of nitrate reductase in
    marine phytoplankton. *Limnology and Oceanography*. 14(2): 194-205.

Everest S.A., Hipkin C.R., and Syrett P.J. 1984. The effect of phosphate and flavin
    adenine dinucleotide on nitrate reductase activity of some unicellular marine
    algae. *Journal of Experimental Marine Biology and Ecology*. 76(3): 263-275.

Ferber L.R., Levine S.N., Lini A., and Livingston G.P. 2004. Do cyanobacteria
    dominate in eutrophic lakes because they fix atmospheric nitrogen?
    Freshwater Biology. 49: 690-708.

Galloway J.N. and Cowling E.B. 2002. Reactive nitrogen and the world: 200 years of
    change. *A Journal of the Human Environment*. 31(2): 64-72.

Glibert P.M. 2017. Eutrophication, harmful algae and biodiversity—Challenging
    paradigms in a world of complex nutrient changes. *Marine Pollution Bulletin*.
    124: 591-606.

Glibert P.M., Beusen A.H.W., Harrison J.A., Dürr H.H., Bouwman A.F., and Laruelle
    G.G. 2018. Changing land-, sea-, and airscapes: Sources of nutrient pollution
    affecting habitat suitability for harmful algae. In: Glibert P.M., Berdalet E.,
    Burford M.A., Pitcher G.C., and Zhou M., editors. Global Ecology and

Oceanography of Harmful Algal Bloooms. Cham, Switzerland: Springer. pp. 53-76.

Glibert P.M., Heil C.A., Hollander D., Revilla M., Hoare A., Alexander J., and Murasko S. 2004. Evidence for dissolved organic nitrogen and phosphorus uptake during a cyanobacterial bloom in Florida Bay. *Marine Ecology Progress Series*. 280: 73-83.

Glibert P.M., Heil C.A., O'Neil J.M., Dennison W.C., and O'Donohue M.J.H. 2006. Nitrogen, phosphorus, silica, and carbon in Moreton Bay, Queensland, Australia: Differential limitation of phytoplankton biomass production. *Estuaries and Coasts*. 29(2): 209-221.

Glibert P.M., Kana T.M., and Brown K. 2013. From limitation to excess: The consequences of substrate excess and stoichiometry for phytoplankton physiology, trophodynamics and biogeochemistry, and the implications for modeling. *Journal of Marine Systems*. 125: 14-28.

Glibert P.M., Manager R., Sobota D.J., and Bouwman L. 2014a. The Haber-Bosch-Harmful algal bloom (HB-HAB) link. *Environmental Research Letters*. 9: 105001.

Glibert P.M., Wilkerson F.P., Dugdale R.C., Parker A.E., Alexander J., Blaser S., and Murasko S., 2014b. Phytoplankton communities from San Francisco Bay Delta respond differently to oxidized and reduced nitrogen substrates—even under conditions that would otherwise suggest nitrogen sufficiency. *Frontiers in Marine Science*. 1:17.

Glibert P.M., Wilkerson F.P., Dugdale R.C., Raven J.A., Dupont C.L., Leavitt P.R.,
Parker A.E., Burkholder J.M., and Kana T.M. 2016. Pluses and minuses of
ammonium and nitrate uptake and assimilation by phytoplankton and
implications for productivity and community composition, with emphasis on
nitrogen-enriched conditions. *Limnology and Oceanography.* 61:165-197.

Harvey H.W. 1953. Synthesis of organic nitrogen and chlorophyll by *Nitzschia
closterium*. *Journal of the Marine Biological Association of the United
Kingdom*. 31(3): 477-487.

Heukelem L.V. and Thomas C.S. 2001. Computer-assisted high-performance liquid
chromatography method development with applications to the isolation and
analysis of phytoplankton pigments. *Journal of Chromatography A*. 910: 31-
49.

Holmes R.M., Aminot A., Kérouel R., Hooker B.A., and Peterson B.J. 1999. A
simple and precise method for measuring ammonium in marine and
freshwater ecosystems. *Canadian Journal of Fisheries and Aquatic Sciences.*
56(10): 1801-1808.

Howarth R., Chan F., Conley D.J., Garnier J., Doney S.C., Marino R., and Billen G.
2011. Coupled biogeochemical cycles: eutrophication and hypoxia in
temperate estuaries and coastal marine ecosystems. *Frontiers in Ecology and
the Environment*. 9(1): 18-26.

Hwang, H. M. and Foster, G. D. 2006. Characterization of polycyclic aromatic
hydrocarbons in urban stormwater runoff flowing into the tidal Anacostia
River, Washington, DC, USA. *Environ. Poll.* 140: 416-426.

Jackson, M. 2016. Phytoplankton and nutrient dynamics with a focus on nitrogen

    form in the Anacostia River, in Washington, D.C. and West Lake, in

    Hangzhou, China. Masters of Science, University of Maryland, College Park,

    MD.

Jeffrey S.W. and Vesk M. 1997. Introduction to marine phytoplankton and their

    pigment signatures. In Jeffrey S.W., Mantoura R.F.C., and Wright S.W. (eds).

    Phytoplankton pigments in oceanography: Guidelines to modern methods.

    Paris: UNESCO.

Lee J., Parker A.E., Wilkerson F.P., and Dugdale R.C. 2015. Uptake and inhibition

    kineatics of nitrogen in *Microcystis aeruginosa*: Results from cultures and

    field assemblages collected in the San Francisco Bay Delta, CA. *Harmful*

    Algae. 47: 126-140.

L'Helguen S., Maguer J.F., and Cardec J. 2008. Inhibition kinetics of nitrate uptake

    by ammonium in size-fractionated oceanic phytoplankton communities:

    Implications for new production and f-ratio estimates. *Journal of Plankton*

    Research. 30(10): 1179-1188.

Lomas M.W. and Glibert P.M. 1999a. Interactions between NH_4^+ and NO_3^- uptake

    and assimilation: Comparison of diatoms and dinoflagellates at several growth

    temperatures. *Marine Biology*. 133: 541-551.

Lomas M.W. and Glibert P.M. 1999b. Temperature regulation of nitrate uptake: A

    novel hypothesis about nitrate uptake and reduction in cool-water diatoms.

    Limnology and Oceanography. 44(3): 556-572.

Lomas M.W. and Glibert P.M. 2000. Comparisons of nitrate uptake, storage, and

    reduction in marine diatoms and flagellates. *Journal of Phycology*. 36: 903-

    913.

MacIsaac J.J., Dugdale R.C., Huntsman S.A., and Conway H.L. 1979. The effect of

    sewage on uptake of inorganic nitrogen and carbon by natural populations of

    marine phytoplankton. *Journal of Marine Resolution*: 37: 51-66.

Miranda K.M., Espey M.G., and Wink D.A. 2001. A rapid, simple

    spectrophotometric method for simultaneous detection of nitrate and nitrite.

    Nitric Oxide. 5(1): 62-71.

Moore L.R., Post A.F., Rocap G., and Chisholm S.W. 2002. Utilization of different

    nitrogen sources by the marine cyanobacteria *Prochlorococcus* and

    Synechococcus. *Limnology and Oceanography*. 47(4): 989-996.

Mooy B.A.S., Fredricks H.F., Pedler B.E., Dyhrman S.T., Karl D.M., Koblízek M.,

    Lomas M.W., Mincer T.J., Moore L.R., Moutin T., Rappé M.S., and Webb

    E.A. 2009. Phytoplankton in the ocean use non-phosphorus lipids in response

    to phosphorus scarcity. *Nature*. 458(7234):69.

Müller S. and Mitrovic S.M. 2015. Phytoplankton co-limitation by nitrogen and

    phosphorus in a shallow reservoir: progressing from the phosphorus limitation

    paradigm. *Hyrdrobiologia*. 744: 255-269.

Nixon S.W. 1995. Coastal marine eutrophication: a definition, social causes, and

    future concerns. *Ophelia.* 41: 199-219.

North R.L., Guildford S.J., Smith R.E.H., Havens S.M., and Twiss M.R. Evidence for phosphorus, nitrogen, and iron colimitation of phytoplankton communities in Lake Erie. *Limnology and Oceanography*. 52(1): 315-328.

O'Neil J.M., Davis T.W., Burford M.A., and Gobler C.J. 2012. The rise of harmful cyanobacteria blooms: The potential roles of eutrophication and climate change. *Harmful Algae.* 14: 313-334.

Parsons T.R., Maita Y., and Lalli C.M. 1984. A Manual of Chemical and Biological Methods for Seawater Analyses. Pergamon Press, New York: 173.

Paerl H.W., Bland P.T., Bowles N.D. and Haibach M.E. 1985. Adaptation to high intensity, low wavelength light among surface blooms of the cyanobacterium *Microcystis aeruginosa*. *Applied Environmental Microbiology*. 49: 1046-1052.

Paerl H.W., Valdes L.M., Joyner A.R., Piehler M.F., and Lebo M.E. 2004. Solving problems resulting from solutions: Evolution of a dual nutrient management strategy for the eutrophying Neuse River Estuary, North Carolina. *Environmental Science & Technology*. 38(11): 3068-3073.

Paerl H.W. Xu H., Hall N.S., Rossignol K.L., Joyner A.R., Zhu G., and Qin B. 2015. Nutrient limitation dynamics examined on a multi-annual scale in Lake Taihu, China: Implications for controlling eutrophication and harmful algal blooms. *Journal of Freshwater Ecology*. 30(1): 5-24.

Paerl H.W., Xu H., McCarthy M.J., Zhu G., Qin B., Li Y., and Gardner W.S. 2011. Controlling harmful cyanobacterial blooms in a hyper-eutrophic lake (Lake

Taihu, China): The need for a dual nutrient (N & P) management strategy. *Water Research*. 45: 1973-1983

Paul V.J. 2008. Global warming and cyanobacterial harmful algal blooms. In: Cyanobacterial Harmful Algal Blooms: State of the Science and Research Needs. Springer, New York, NY, 2008. p. 239-257.

Probyn T.A. and Painting S.J. 1985. Nitrogen uptake by size-fractionated phytoplankton populations in Antarctic surface waters. *Limnology and Oceanography*. 30(6): 1327-1332.

Raven J.A., Willenweber B., and Handley L.L. 1992. A comparison of ammonium and nitrate as nitrogen sources for photolithotrophs. *New Phytologist*. 121: 19-32.

Revilla M., Alexander J., and Glibert P.M. 2005. Urea analysis in coastal waters: Comparison of enzymatic and direct methods. *Limnology and Oceanography*. 3: 290-299.

Reynolds C.S. 1999. Non-determinism to probability, or N:P in the community ecology of phytoplankton. *Arch. Hydrobiol.* 146: 23-35.

R Core Team. 2014. R: A language and environment for statistical computing. R Foundation for Statistical Computing. R Foundation for Statistical Computing, Vienna, Austria.

Shangguan Y., Glibert P.M., Alexander J.A., Madden C.J., and Murasko S. 2017a. Nutrients and phytoplankton in semienclosed lagoon systems in Florida Bay and their responses to changes in flow from Everglades restoration. *Limnology and Oceanography*. 62: S327-S347.

Shangguan Y., Glibert P.M., Alexander J.A., Madden C.J., and Murasko S. 2017b.

    Phytoplankton assemblage response to changing nutrients in Florida Bay:

    Results of mesocosm studies. *Journal of Experimental Marine Biology and*

    Ecology. 494: 38-53.

Solomon, C.M., Jackson M., Glibert P.M., and G. Vazquez. 2019. Chesapeake Bay's

    'forgotten' Anacostia River: Eutrophication status and nutrient reduction

    measures. *Environmental Monitoring and Assessment.* 91: 265.

Song B. and Ward B.B. 2007. Molecular cloning and characterization of high-affinity

    nitrate transporters in marine phytoplankton. *Journal of Phycology*. 43: 542-

    552.

Swarbrick V.J., Simpson G.L., Glibert P.M., and Leavitt P.R. 2019. Differential

    stimulation and suppression of phytoplankton growth by ammonium

    enrichment in eutrophic hardwater lakes over 16 years. *Limnology and*

    Oceanography. 64: S130-S149.

Syrett P.J. 1981. Nitrogen metabolism of microalgae. *Canadian Bulletin of Fisheries*

    and Aquatic Sciences. 210: 182-210.

Van Heukelem L. and Thomas C.S. 2001. Computer-assisted high-performance liquid

    chromatography method development with applications to the isolation and

    analysis of phytoplankton pigments. *Journal of Chromatography A*. 910: 31-

    49.

Van Heukelem L. and Thomas C.S. 2005. The HPL Method. In: Hooker S.B., Van

    Heukelem L., Thomas C.S., Claustre H., Ras J., Barlow R., Sessions H.,

    Schlüter L., Perl J., Trees C., Stuart V., Head E., Clementson L., Fiskwick J.,

Llewellyn C., and Aiken J., eds. The second SeaWiFs HPLC analysis round-
robin experiment (SeaHARRE-2). NASA Tech. Memo. pp. 86-92.

Waiser M.J., Tumber V., and Holm J. 2011. Effluent-dominated streams. Part 1:
Presence and effects of excess nitrogen and phosphorus in Wascana Creek,
Saskatchewan, Canada. *Environmental Toxicology and Chemistry*. 30(2): 496-
507.

Wright S. W., Jeffrey S. W., and Mantoura, R. F. C. Eds. 2005. Phytoplankton
pigments in oceanography: guidelines to modern methods. Unesco Pub.

Xu J., Glibert P.M., Liu H., Yin K., Yuan X., Chem M., and Harrison P.J. 2012.
Nitrogen sources and rates of phytoplankton uptake in different regions of
Hong Kong waters in summer. *Estuaries and Coasts*. 35: 559-571.

Xu H., Paerl H.W., Qin B., Zhu G., Hall N.S., and Wu Y. 2014. Determining critical
nutrient thresholds needed to control harmful cyanobacterial blooms in
eutrophic Lake Taihu, China. *Environmental Science & Technology*. 49:
1051-1059.

Yoshiyama K. and Sharp J.H. 2006. Phytoplankton response to nutrient enrichment in
an urbanized estuary: Apparent inhibition of primary production by
overeutrophication. *Limnology and Oceanography*. 51(1, part 2): 424-434.

Zimmerman, C., Price, M. and Montgomery, J. 1977. Operation, Methods and
Quality Control of Technicon AutoAnalyzer II Systems for Nutrient
Determination in Seawater. Harbor Branch Foundation, Inc., Technical
Report No.11. Harbor Branch Foundation, Inc., Fort Pierce, Florida.

Zohary T., Herut B., Krom M.D., Mantoura F.C., Pitta P., Psarra S., Rassoulzadegan
F., Stambler N., Tanaka T., Thingstad T.F., and Woodward E.M.S. 2005. P-
limited bacteria but N and P co-limited phytoplankton in the Eastern
Mediterranean—a microcosm experiment. *Deep Sea Research II.* 52: 3011-
3023.

Chapter 3: Nutrient effects on photosynthesis, nitrate reductase activity, silicification and gene expression in the diatom *Thalassiosira pseudonana* across a broad temperature gradient

Abstract

Diatom cells utilize a variety of metabolic pathways to cope with internal energy imbalances caused by stressful environmental conditions. In this study, the model diatom species, *Thalassiosira pseudonana,* was grown in nitrate (NO_3^-) and dissolved silicate (Si)-depleted media across a temperature gradient (4, 17, 28 °C) to determine how nutrient enrichment and temperature stress would affect diatom growth, photosynthesis, nitrate reductase (NR) enzyme activity, biogenic silica ($bSiO_2$) deposition, and gene expression. Cells grown at 4 °C under nutrient-replete conditions had significantly higher $bSiO_2$ deposition rates than cells grown at 17 and 28 °C. The relative expression of the targeted NR gene was on average ~10 times higher in the 4 °C cultures and ~4 times higher in the 28 °C than in the 17 °C cultures, while the activity of the NR enzyme was generally highest in the cultures grown at 17 °C that were enriched with NO_3^-. Across all nutrient treatments, the cells grown at 17 °C had an average Fv/Fm was of 0.44, while the cells grown at 4 °C and 28 °C had an average Fv/Fm of 0.37 and 0.38 respectively. The physiological responses highlighted here demonstrate how water temperature and nutrient limitation may stress diatom cells and how the mechanisms diatoms use to cope with such stressors impact the growth, physiology, and morphology of these primary producers.

Introduction

Diatoms make substantial contributions to new production in marine and freshwater ecosystems and have been estimated to fix over 10 billion tons of inorganic carbon (C) in the oceans each year (Goldman 1993, Del Amo et al. 1997, Brzezinski et al. 1998, Smetacek 1998, Granum et al. 2005). In addition to the significant role that diatoms play in global primary production, these organisms are also important in the export of C from the euphotic zone and in the biogeochemical cycling of nutrients in aquatic ecosystems (Round et al. 1990, Raven and Falkowski 1999, Ragueneau et al. 2006). Although diatoms are widely distributed and appear to be "cosmopolitan" in nature (Finlay and Fenchel 2004), they do have environmental preferences and changes in the surrounding environment can stress diatom cells and impact the subsequent growth and productivity of these primary producers.

Diatoms often dominate phytoplankton assemblages during the onset of spring blooms and in upwelling regions when waters are cool, nutrient-rich, and weakly stratified (Cushing 1989, Peinert et al. 1989, Eppley et al. 1969b, Lomas and Glibert 1999a). Following spring freshets and upwelling events, waters that are injected into the euphotic zone are typically rich in nitrate (NO_3^-) and dissolved silicate (Si), both of which may help fuel diatom blooms (Dugdale 1985). The availability of oxidized NO_3^- relative to chemically-reduced nitrogen (N) forms (e.g., NH_4^+), can also play an important role in diatom growth and productivity because diatoms often prefer NO_3^- over NH_4^+ (Probyn and Painting 1985, Lomas and Glibert 1999a, Glibert et al. 2016). Given that Si is necessary for diatom cells to divide, and the general preference for NO_3^- by diatoms, the relative availability of Si and NO_3^- may influence diatom abundance.

However, even when essential nutrients are readily available in the water column, other environmental factors such as water temperature may affect diatom growth and productivity. Water temperature becomes an important controlling variable when the pathways of N and C assimilation become uncoupled. Typically, the light-dependent reactions of photosynthesis are unaffected by temperature, while the Calvin cycle, responsible for C assimilation, slows down as temperatures decrease (Kok 1956, Falkowski and Raven 1997). The Calvin cycle enzyme Rubisco is responsible for the first step of C fixation and typically has a temperature optimum of ~30 °C or greater (Li 1980, Smith and Platt 1985, Ras et al. 2013). In contrast, the nitrate reductase (NR) enzyme that is responsible for catalyzing the reduction of NO_3^- to NO_2^- has been found to operate optimally when temperatures are cool (~10-20 °C; Lomas and Glibert 1999a, Gao et al. 2000, Berges et al. 2002). If Rubisco activity declines as temperatures decrease, excess reductant may build up from the biophysical light reactions which can lead to photodamage or photoinhibition (Falkowski and Raven 1997, Sobrino and Neale 2007, Glibert et al. 2016). In order to overcome this imbalance, diatoms have been shown to reduce NO_3^- to nitrite (NO_2^-) in a non-assimilatory fashion (Lomas and Glibert 1999a,b, Glibert et al. 2016) thus making dissimilatory NO_3^- reduction an efficient energy dissipation pathway when temperatures are cool and the NR enzyme is operating efficiently. However, at temperatures well below ~10 °C and well above ~20 °C, the efficiency of dissimilatory NO_3^- reduction may decrease. Therefore, overflow pathways other than dissimilatory NO_3^- reduction may be necessary for diatom cells to overcome internal energy imbalances that occur when photochemistry and C fixation become

56

uncoupled. Photorespiration is one such pathway (Huner et al. 1998, Parker and Armbrust 2005, Glibert et al. 2016). As a whole, photorespiration is an energetically inefficient process that results in a net loss of C fixation; however, increases in photorespiration may work to alleviate the stress that diatoms experience when photochemistry and C fixation become uncoupled (Parker and Armbrust 2005, Glibert et al. 2016).

It has been suggested that increases in photorespiration may stimulate mitochondrial urea cycle activity that is, in turn, related to the synthesis of polyamine proteins in diatom cells (Liu and Glibert 2018). These polyamine proteins are incorporated into the silaffin proteins that are responsible for biogenic silica ($bSiO_2$) deposition in diatom cell walls (Sumper and Kröger 2004). Therefore, if increases in photorespiration stimulate urea cycle activity and lead to increases in polyamine synthesis, silicification may increase (Liu and Glibert 2018). Heavily silicified diatoms have a greater propensity for sinking, which may lead to increased $bSiO_2$ export from the photic zone (e.g., Dugdale et al.1995). Thus, the degree of silicification can affect the rates of dissolution and biogeochemical cycling of $bSiO_2$, altering the subsequent availability of Si to diatoms in the water column (Liu and Glibert 2018).

The goal of this study was to use the model diatom species, *Thalassiosira pseudonana*, to quantify the relationships between nutrient availability, photosynthesis, NR enzyme activity, silicification, and NR gene expression when cells were growing at three temperatures: at or near the presumed NR temperature optima (17 °C), well above it and near the optimal temperature for Rubisco (28 °C),

and well below the optimal temperature of both enzymes (4 °C). It was hypothesized that diatom photosynthesis, NR enzyme activity and NR gene expression should increase when temperatures are near the NR temperature optima and when NO_3^- and Si are readily available in the surrounding media. In contrast, cold, nutrient-replete conditions should increase photochemical stress in diatom cells and should lead to decreases in NR activity and gene expression and increases in cell wall silicification. The information obtained through this study may begin to elucidate how metabolic energy balance and overflow pathways function in this diatom species under different temperature and nutrient conditions.

Materials and Methods

Culture Conditions and Experimental Design

A culture of *T. pseudonana* CCMP 1335 was obtained from the Horn Point Laboratory Oyster Hatchery and was grown in f/2 culture media (Guillard 1983). Cultures were acclimated to three temperatures, 4 °C, 17 °C, and 28 °C over the course of several weeks to months and were maintained in batch conditions under a 12:12 light:dark cycle at a light level of ~200 µE m^{-2} s^{-1}, gently bubbled with CO_2. To initiate experiments, *T. pseudonana* cultures were transferred into new glass containers with fresh f/2 media and the growth of the cells in the cultures were monitored using a BD Accuri C6 flow cytometer. When the cultures were in the exponential phase of growth, cells were concentrated by filtration or centrifugation and were transferred into replicated 2-liter culture flasks that contained NO_3^- and Si-depleted media.

Cell growth in the nutrient-depleted cultures was monitored until the cells in these nutrient-depleted cultures reached stationary phase (residual nutrient permitted short-term growth). On the first day that a decline in growth rate was noted, 500 mL of each nutrient-depleted culture were transferred into 8 separate polyethylene culture flasks. Duplicate flasks were then enriched with 3 different combinations of nutrients (Table 1). Additions of either NO_3^- and/or Si were made at 100 μM (Table 1). Control flasks received no added nutrients.

Immediately after making the nutrient additions, and again 24 hours later, aliquots were removed from the cultures for measurements of cell abundance, concentrations of NO_3^- and Si, variable fluorescence characteristics, NR enzyme activity, $bSiO_2$ deposition, and the relative expression of genes that are associated with NR activity and silification.

Cell abundance quantification

To quantify cell abundance in each of the experimental containers, 1.5 mL of each culture were fixed with 10% paraformaldehyde and stored at 4 °C until analysis. Cell counts were then obtained using a BD Accuri C6 flow cytometer with dual excitation (488 nm, 640 nm). When analyzed on the flow cytometer, cells were gated by shape and size using forward scatter and side scatter settings. Cell concentrations were calculated by dividing absolute cell counts by the volume of sample that was analyzed.

Nutrient analyses

Aliquots of media from all flasks were filtered through precombusted GF/F filters, and the filtrate was frozen at -18 °C until nutrient analyses were performed.

Concentrations of NO_3^- were determined according to Miranda et al. (2001) and

Doane and Horwáth (2003). Concentrations of Si were determined at Horn Point

Analytical Services Laboratory according to Zimmerman et al. (1977).

PAM fluorometry

Variable fluorescence parameters were obtained using a Waltz Phyto-PAM II

fluorometer. At each sampling time, 2 mL of each culture treatment were collected

and placed in a glass test tube. The samples were then placed in darkness for 15-20

minutes. After the dark incubation period, the algal quantum efficiency (Fv/Fm), light

saturation parameter (E_k), initial slope (α), and maximum electron transport rate

(ETR_{max}) were measured.

Nitrate reductase activity

The activity of NR enzyme was measured using the NO_3^- reduction protocol

of Eppley et al. (1969a) as modified by Berges and Harrison (1995). Aliquots of 25

mL were first filtered onto a precombusted GF/F filter, then flash frozen and stored at

-80 °C until analysis. After no more than 1 week in the freezer, the frozen GF/F filters

were homogenized in a glass Teflon homogenizer with 3.3 mL of extraction buffer.

The extraction buffer contained 1 mM of dithiothreitol, 5 mM EDTA, 0.2 M

phosphate buffer, 0.1% v/v Triton X-100, and 0.3% w/v polyvinyl pyrrolidone, and

was adjusted to a pH of ~8 using potassium hydroxide pellets. The homogenized filter

material was centrifuged for 5 minutes at 4 °C and 3000 rpm. Then, the supernatant

was divided into 2, 1 mL portions, one of which was used as a control and one was

used for the NO_3^- reduction reaction. The control and reaction tubes were all

incubated at their respective experimental growth temperatures (4, 17, or 28 °C) for

30 minutes. The control tubes were incubated with 0.2 M $NaNO_3^-$, 0.05 M $MgSO_4^-$, and 300 μL extraction buffer, and the treatment tubes were incubated with 0.2 M $NaNO_3^-$, 0.05 M $MgSO_4^-$, and 300 μL of 150 μM NADH. The reactions were stopped by adding 1M zinc acetate and 5 mL of 95% ethanol. The samples were then centrifuged for 5 minutes at 15 °C and 3000 rpm. Excess NADH was oxidized by adding 0.83 μM phenazine methosulfate to the supernatant obtained by centrifugation. Then, the supernatant was used to determine NO_2^- formation in each of the samples.

The concentration of NO_2^- formed in each of the samples was quantified spectrophotometrically (Eppley et al. 1969a; Parsons et al. 1984). To determine NO_2^- concentrations in each of the samples, 800 μL of supernatant was combined with 32 μL of the color detection reagent. Following color development, absorbance readings were measured at 543 nm on a BioTek Synergy HT or a BioTek Synergy LX plate reader. The NR activity values were normalized to cell abundance to determine NR activity cell^{-1} hour^{-1}.

Silica deposition rate

For measurements of silicification, the fluorescent analog, 2-(4-pyridyl)-5-((4-(2- dimethylaminoethylaminocarbamoyl)methoxy)phenyl)oxazole (PDMPO), was used. This compound is incorporated into diatom cell walls at a constant ratio with $bSiO_2$ (Shimizu et al. 2001, McNair et al. 2015). PDMPO was added to subsamples of the *T. pseudonana* cultures so that the final concentration of PDMPO in each bottle was 0.157 μM. The bottles were incubated at the temperature of culture growth (4, 17, or 28 °C) for 24 hours and samples were subsequently analyzed according to

61

McNair et al. (2015) and Shimizu et al. (2001). First, the cells in each container were filtered onto a 14 mm polycarbonate filter, placed in a 15 mL polyethylene tube, covered with 10 mL 100% methanol, and placed in the dark at 4 °C for 24 hours. Following the 24-hour incubation, the filters were compressed at the bottom of the tube using a Teflon rod and the tubes were centrifuged for 10 minutes at 2500 rpm. Then, 9 mL of the methanol were removed from each tube and the tubes were left to dry (uncapped) in a 50 °C oven. Once the filters were dry, 200 µL of 0.5 M hydrofluoric acid (HF) were added to each tube and the tube was mixed using a Teflon rod. The tubes with HF were incubated for 3 hours. Then, 2.8 mL of 1 M boric acid were added to each of the tubes and 1 mL was transferred into a cuvette with 2 mL of 100% methanol. Fluorescence measurements were obtained using a FluoroMax fluorometer (excitation: 365/30, emission: 534/30) and were compared to a standard curve consisting of PDMPO in a matrix of HF and boric acid. The concentration $bSiO_2$ deposited into the culture cells was estimated using a $bSiO_2$:PDMPO ratio of 2,900:1 when the silicic acid ($Si(OH)_4$) concentration was greater than 3 µM and using the equation $bSiO_2$:PDMPO $= 912.6 * [Si(OH)_4]$ when the concentration of $Si(OH)_4$ was less than 3 µM (McNair et al. 2015).

Gene expression analysis

Two genes were targeted for differential gene expression analysis, a NR gene and a silaffin gene (TPSIL2). Primers used to target the NR gene were obtained from Parker and Armbrust (2005) and those used to amplify the silaffin gene were designed using the default settings in the NCBI Primer Blast program (Ye et al. 2012, Table 2). To quantify differential expression, actin was used as a housekeeping gene,

and those primers were obtained from McGinn and Morel (2008). The PCR products that resulted from the differential expression analyses were run on a 1% agarose gel to confirm that the primers used were specific and that the target sequences were properly amplified. The primers that were designed to target the silaffin gene were not specific across all PCR runs. Due to this lack of specificity, the silaffin gene expression data were not included in subsequent analyses.

To extract total RNA, ~50 mL of culture were filtered onto a Supor-200 membrane filter. Cells captured on the filter were scraped into a clean microcentrifuge tube, lysed using a pestle, and flash frozen in liquid N_2. Total RNA from the cells was extracted using the Qiagan RNeasy Plant Mini Kit. The total RNA that was obtained from each RNA extraction was incubated with Invitrogen DNase I to ensure that genomic DNA was not a source of contamination in the subsequent analyses. Following the RNA extraction and DNA digestion protocols, total RNA was quantified using a Qubit RNA HS Assay Kit. The total RNA obtained from each culture was stored at -80 °C until RT-qPCR procedures were performed.

Following RNA quantification, the RT-qPCR analyses were conducted using the Qiagen one-step QuantiNova SYBR Green RT-PCR Kit. To run the RT-qPCR analysis, 5 µL of total RNA were added to a mixture containing 10 µL 2x SYBR Green RT-PCR Master Mix, 0.2 µL QN SYBR Green RT-Mix, 1 µL of both the forward and reverse primers (10µM), and 2.8 µL of RNase-free water, for a total reaction volume of 20 µL. The reaction mixtures were then run on a Bio-Rad CFX96 qPCR machine. The first reverse transcription step of the reaction was 50 °C for 10

min. Following reverse transcription, the PCR reaction proceeded at 95 °C for 2 min, followed by 40 cycles at 95 °C for 5 s and 60 °C for 10 s.

After the RT-qPCR reactions, the mean cycle threshold (C^t) value of actin obtained for each sample was plotted as a function of the concentration of RNA measured in each sample to confirm that actin was constitutively expressed across all treatments and temperatures. Then, the expression of the NR gene relative to the expression of the actin gene was calculated as relative transcript abundance = $2^{(\Delta Ct)}$ (Pfaffl 2007).

Statistical Analyses

To determine the main and interactive effects of temperature and nutrient limitation, two-way ANOVA analyses were conducted using the programming software R (R Core Team 2014) with temperature and treatment (nutrient addition) as the two independent factors. The dependent variables examined through these analyses were algal Fv/Fm, ETR_{max}, NR activity, $bSiO_2$ deposition (PDMPO incorporation), and relative NR gene expression. In addition, one-way ANOVA analyses were used to examine the effects that growth temperature and nutrient addition alone had on the physiological and gene expression measurements. Tukey's post-hoc tests were used to determine significant differences between the growth temperature and nutrient treatments.

Results

Algal growth rates and nutrient concentrations

The highest growth rates were observed at 17 °C and the lowest growth rates were observed at 4 °C in the nutrient-replete culture bottles (Fig. 1). Growth rates in

64

exponential conditions were 0.41, 1.28, and 0.66 day^{-1} for the 4, 17, and 28 °C

cultures respectively. After cells were transferred to NO_3^- and Si-depleted media, the

growth rates of the 28 °C cultures were significantly higher than the growth rates of

the 4 and 17 °C cultures (one-way ANOVA/Tukey's HSD, $p < 0.01$ and $p < 0.05$

respectively). Additionally, the growth rates noted in the 17 °C cultures were

significantly higher than those noted in the 4 °C cultures (one-way ANOVA/Tukey's

HSD, $p < 0.01$). The average algal growth rates in the nutrient-depleted cultures were

0.50 ± 0.01 day^{-1} at 4 °C, 0.91 ± 0.01 day^{-1} at 17 °C, and 1.08 ± 0.06 day^{-1} at 28 °C

(Fig. 1).

As expected, following nutrient enrichment, the concentrations of NO_3^- and Si

in the NO_3^--enriched and Si-enriched cultures were significantly higher than the

concentrations of these respective nutrients in cultures that did not receive such

enrichments (Wilcoxon rank sum test, $p < 0.01$).

PAM analyses

The fluorometric analyses revealed that immediately following nutrient

enrichment there was no significant effect of temperature or nutrient enrichment on

the Fv/Fm of the *T. pseudonana* cells (two-way ANOVA, Fig. 2). Although growth

and incubation temperature did not significantly alter algal Fv/Fm at either

experimental time point, the Fv/Fm values of the 17 °C cultures were consistently

higher than those of the 4 and 28 °C cultures. After 24 hours of incubation with

nutrients, the average Fv/Fm values of the cultures were 0.36 ± 0.02 at 4 °C, $0.44 \pm$

0.03 at 17 °C, and 0.37 ± 0.07 at 28 °C.

There were some significant effects of nutrient enrichment on algal Fv/Fm in cultures that were grown at 4 °C and 28 °C (one-way ANOVA). After 24 hours of incubation with nutrients at 4 °C, the control, NO_3^-, and NO_3^- + Si-enriched cultures had significantly higher Fv/Fm values than the cultures that were enriched with Si alone (Tukey's HSD, $p < 0.05$, $p < 0.05$, and $p < 0.01$ respectively). In the cultures that were incubated at 28 °C, the Fv/Fm values were significantly higher in the cultures that were enriched with NO_3^- and NO_3^- + Si than in the cultures that were not enriched with NO_3^- (Tukey's HSD, all relationships $p < 0.01$). While algal Fv/Fm was significantly affected by nutrient enrichment after 24-hours at 4 and 28 °C, the Fv/Fm values of cultures that were grown and incubated at 17 °C were not significantly altered by nutrient enrichment.

The temperature at which the *T. pseudonana* cultures were grown had a significant effect on the ETR_{max} values obtained for the cultures immediately following nutrient addition and 24 hours after nutrient addition ($p < 0.01$ for both time points, Fig. 3). At the initial time point after nutrient enrichment, the cultures had an average ETR_{max} of 25.05 ± 2.1, 20.8 ± 0.9 , and 8.9 ± 1.2 μmol electrons m^{-2} s^{-1} at 4, 17 and 28 °C, respectively. Then, 24 hours following nutrient enrichment, the average ETR_{max} values were 23.9 ± 3.9, 22.1 ± 7.0 , and 6.24 ± 1.5 μmol electrons m^{-2} s^{-1} at the respective temperatures. There was also a near-significant effect of nutrient enrichment on algal ETR_{max} after 24 hours of incubation with nutrients ($p = 0.062$). In general, the NO_3^- and NO_3^- + Si enriched treatments had higher ETR_{max} values than the Si-enriched and control treatments after 24 hours of incubation (Fig. 3).

When looking at the effects of nutrient enrichment on ETR_{max} at each growth temperature, some significant trends emerged. At 4 °C, the cultures that were enriched with NO_3^- alone had a significantly higher ETR_{max} after 24 hours than the control cultures or the cultures that were enriched with Si alone (one-way ANOVA/Tukey's HSD, $p < 0.05$ for both relationships). Additionally, at 28 °C, the cultures that were enriched with $NO_3^- + Si$ had a significantly higher ETR_{max} after 24 hours of incubation than the control cultures and the cultures that were enriched with Si alone (one-way ANOVA/Tukey's HSD, $p < 0.05$ for both relationships). At 17 °C, nutrient enrichment did not have any significant effect on algal ETR_{max}.

NR activity analysis

There was no significant effect of temperature or nutrient treatment on the activity of the NR enzyme even though there were differences between treatments ($p = 0.83$ and $p = 0.14$ for temperature and treatment respectively; Fig. 4). The average activity of the NR enzyme was typically highest at 17 °C and lowest at 28 °C. Immediately following nutrient enrichment, the average activities of the NR enzyme were 2.34 ± 2.25, 9.57 ± 4.46, and 2.05 ± 1.09 fmol NO_2^- formed cell^{-1} hour^{-1} at 4, 17 and 28 °C, respectively. Then, after 24 hours of incubation with nutrients, the average activity of the NR enzyme declined in all of the 17 °C *T. pseudonana* cultures. The average activities of the NR enzyme after 24 hours were 3.61 ± 2.37, 7.54 ± 3.84, and 2.69 ± 1.53 fmol NO_2^- formed cell^{-1} hour^{-1} at 4, 17 and 28 °C. Additionally, the 17 °C cultures that were enriched with NO_3^- or $NO_3^- + Si$ had higher average NR values than the control and Si-enriched culture immediately following nutrient enrichment. After enrichment, the average activity of the NR enzyme was 6.87 ± 5.34 fmol NO_2^-

formed cell^{-1} hour^{-1} for the NO_3^- and NO_3^- + Si treatments and 3.25 ± 3.08 fmol NO_2^- formed cell^{-1} hour^{-1} for the control and Si treatments.

PDMPO incorporation

The PDMPO incorporation technique revealed that temperature and nutrient enrichment in isolation and in combination with one another had a significant effect on $bSiO_2$ deposition (two-way ANOVA, nutrient enrichment: $p < 0.01$, temperature: $p < 0.05$, nutrient enrichment x temperature: $p < 0.01$, Fig. 5). When the cells in culture were incubated with PDMPO 24 hours after nutrient enrichment, there was a significant effect of nutrient enrichment on $bSiO_2$ deposition (one-way ANOVA, $p < 0.01$) and a significant, interactive effect of temperature and nutrient addition on $bSiO_2$ deposition (two-way ANOVA, $p < 0.05$).

Nutrient enrichment had a significant effect on $bSiO_2$ deposition (One-way ANOVA). At both the initial and final time points, the cultures that were enriched with NO_3^- + Si had significantly higher $bSiO_2$ deposition rates than rates associated with the control and NO_3^- treatments (Tukey's HSD, $p < 0.01$ for all comparisons). When the cultures were incubated with PDMPO immediately following nutrient addition, the highest $bSiO_2$ deposition values were noted in the 4 °C NO_3^- + Si-enriched cultures (6.08 ± 1.52 pmol $bSiO_2$ deposited cell^{-1} hour^{-1}) and the lowest $bSiO_2$ deposition values were noted in the 28 °C control cultures (0.065 ± 0.041 pmol $bSiO_2$ deposited cell^{-1} hour^{-1}). When the cultures were incubated with PDMPO 24 hours after nutrient enrichment, the highest $bSiO_2$ deposition values were still noted in the 4 °C NO_3^- + Si-enriched cultures (4.47 ± 1.27 pmol $bSiO_2$ deposited cell^{-1}

hour^{-1}), while the lowest bSiO$_2$ deposition values were noted in the 4 °C control

cultures (0.069 ± 0.029 pmol bSiO$_2$ deposited cell^{-1} hour^{-1}, Fig. 5).

Gene expression analyses

There was a significant effect of both temperature and nutrient enrichment on

the relative expression of the NR gene immediately following nutrient addition in the

T. pseudonana cultures (Fig. 6). The relative expression of the NR gene was

significantly greater in the cultures that were grown at 4 °C than in those that were

grown at 17 °C (one-way ANOVA/Tukey's HSD, $p < 0.01$). The cultures that were

grown at 4 °C also tended to have higher relative NR expression than the cultures that

were grown at 28 °C, though this relationship was not statistically significant ($p =$

0.06). In the cultures that were grown at 4 °C, the relative expression of the NR gene

was significantly altered by all nutrient enrichment treatments (one-way

ANOVA/Tukey's HSD, $p < 0.01$ for all comparisons).

Discussion

The overarching goal of this study was to determine how nutrient availability

and water temperature impact diatom growth, photosynthesis, NR activity, and gene

expression. As to be expected, both nutrient availability and temperature influenced

the growth rates and biomass of the *T. pseudonana* cells in culture. Additionally,

differences in nutrient availability and temperature impacted *T. pseudonana* variable

fluorescence characteristics, bSiO$_2$ deposition, and NR gene expression. Together,

information obtained through this study underscores that although diatoms are

resilient and may be sustained under a variety of temperature and nutrient conditions,

moderate temperatures and nutrient-rich waters increase the physiological

performance of diatom cells. Additionally, the results obtained in this experiment support the hypothesis that cold, nutrient-replete conditions lead to increases in diatom cell wall silicification. Lastly, this study suggests that NR enzyme activity may be regulated downstream of mRNA transcription under specific environmental conditions.

$bSiO_2$ deposition as a result of diatom stress response

The results of this study support the physiological mechanism outlined by Liu and Glibert (2018) that links cold water temperatures to increased silicification in at least some diatom taxa. In their proposed mechanism, Liu and Glibert (2018) suggest that under cold temperature and high-light conditions, diatom cells experience stress and may become more heavily silicified. The results of this study support the idea that growth at cold (~ 4 °C) temperatures is stressful based on the Fv/Fm data obtained through fluorometric analyses (Fig. 2). The lower Fv/Fm values that were noted in the 4 °C cultures suggest that the cells growing at 4 °C may have been limited or stressed to some degree (Falkowski et al. 1992), though the intricate imbalances in metabolism that may have occurred at the cellular level were not accounted for in this study. Liu and Glibert (2018) discuss photorespiration as a mechanism for coping with imbalances in cellular metabolism that may be apparent under cold temperature conditions and link increases in photorespiration to increases in mitochondrial urea cycle activity, increases in polyamine synthesis, and increases in diatom cell wall silicification. While rates of photorespiration and urea cycle activity were not measured in this study, $bSiO_2$ deposition rates were measured and were influenced by both diatom growth temperature and nutrient availability (Fig. 5).

The results of this study revealed that $bSiO_2$ deposition was highest when *T. pseudonana* cells were grown and incubated at 4 °C and when cells were supplied with NO_3^- and Si at approximately a 1:1 ratio, thus supporting the hypothesis that cold, nutrient-replete waters may promote silicification in diatom cells.

In general, the effects of temperature and nutrient limitation on diatom $bSiO_2$ deposition have not been studied in detail, however, a previous laboratory study conducted by Durbin (1977) found that the amount of intracellular Si per unit surface area in *Thalassiosira nordenskioeldii* was ~2 times greater in cells grown at 0 °C than in cells grown at 10 °C under nutrient-replete conditions. Similarly, in a study conducted by Paasche (1980), the Si content per diatom cell increased with decreasing temperatures (8-23 °C) in the diatoms *Chaetoceros affinis* and *Rhizosolenia fragilissima*. In a study conducted Spilling et al. (2015), the amount of Si relative to C in Si-limited *Chaetoceros wighamii* cells was greater when cells were grown at 7 °C as opposed to 11 °C under moderate (130 μmol photos m^{-2} s^{-1}) light conditions. In a more recent study conducted by Lomas et al. (2019), a number of polar diatom species were isolated and maintained under low temperature conditions (~2 °C) to determine how these colder temperatures would affect the Si content per diatom cell as a function of cell biovolume. The results of the Lomas et al. (2019) study revealed that the amount of Si per diatom cell increased with cell biovolume 5-15 times more in the cells grown at cold temperatures than in diatom cells from other studies that were grown under temperate conditions (Fig. 3b, Lomas et al. 2019). Together, the results herein and those of Durbin (1977), Paasche (1980),

Spilling et al. (2015), and Lomas et al. (2019) broadly agree that colder temperature conditions may promote higher frustule Si content in certain diatom species.

A number of field studies have also noted increases in the abundance of heavily silicified diatom species under cold temperature conditions. For example, in Sishili Bay, China, an increase in the abundance of the small, heavily silicified diatom *Paralia sulcata* has been noted in recent years with increases in eutrophication and increases in N relative to Si (Liu et al. 2013, Liu and Glibert 2018). Similarly, increases in the abundance of smaller diatoms with thicker frustules have been noted in the Baltic Sea during the winter and early spring season (Wasmund et al. 1998). A study conducted by Baines et al. (2010) compared diatom silicification in the cold, nutrient-replete waters of the Antarctic Zone of the Southern Ocean (SOAZ) to the warm, nutrient-depleted waters of the Eastern Equatorial Pacific (EEP). The results of that study revealed that diatoms living in the colder waters of the SOAZ had ~6 times more $bSiO_2$ per unit volume than the diatoms living in the EEP waters (Baines et al. 2010), suggesting that both nutrient availability and temperature may play a role in altering diatom cell wall thickness in these regions. Similarly, in a study conducted by Takeda (1998), Si consumption by diatoms was 2 times greater in the high-latitude waters of the Southern Ocean and the Subarctic North Pacific than they were for the low-latitude waters of the Equatorial Pacific. Together, these field observations support the notion that colder waters may lead to increased silicification in diatom cells, though the intricate physiological processes underlying these differences in silicification may need to be explored in more detail.

The results presented here suggest that colder temperatures and elevated N:Si conditions may lead to increased $bSiO_2$ deposition in diatom cells. If environmental shifts indeed select for diatom cells with thicker frustules, such changes in phytoplankton ecology may in turn impact the overall biogeochemical cycling of Si in an aquatic ecosystem (Liu and Glibert 2018). For example, it has been suggested that heavily silicified diatoms sink faster than less silicified forms and may lead to increased $bSiO_2$ sequestration in the sediments (Dugdale et al. 1995, Liu et al. 2013, Liu and Glibert 2018). Increased nutrient sequestration can slow down the rate of $bSiO_2$ dissolution in the sediments and may impact the subsequent availability of Si relative to other essential nutrients in the water column, especially because N and phosphorus (P) are remineralized relatively quickly compared to $bSiO_2$ (Officer and Ryther 1980, Martin-Jézéquel et al. 2000, Liu et al. 2013). Such changes in the relative availability of Si over time may promote the growth of non-silicious and potentially harmful phytoplankton species (Anderson et al. 2002, Liu and Glibert 2018).

Nitrate reductase enzyme activity and gene expression

The variability noted in NR enzyme activity, and therefore non-statistically significant results, may be due to inherent analytical variability with this assay. Only 2 replicates were used in this study. Despite the fact that the activity of the NR enzyme was not significantly affected by temperature, the activity of this enzyme was generally higher at 17 °C than it was at the cold and hot temperature extremes (Figure 4). Conversely, the relative expression of the NR gene targeted in this study was significantly affected by temperature and was lower in the cultures that were grown at

17 °C than in the cultures grown at 4 or 28 °C (Figure 6). These results differ from a previous study conducted by Parker and Armbrust (2005) in which the number of copies of NR mRNA in *T. pseudonana* cells grown at a higher growth temperature (22 °C) was less than that of cells grown at a more moderate growth temperature (12 °C) when cells were exposed to high-light conditions. Although the data obtained in this study seem to contradict the data reported by Parker and Armbrust (2005), the extreme temperature and nutrient-limitation conditions that the cells in this study were subject to may have influenced the NR expression data obtained. Importantly, in the Parker and Armbrust (2005) study, the ratio of the NR mRNA copy number to the mRNA copy number of a gene involved in photorespiration (phosphoglycolate phosphatase; PGP) was higher when cells were grown at a warmer (22 °C) temperature. This increase in the NR mRNA: PGP mRNA ratio suggests that cells growing at a warmer temperature may upregulate NR genes in order to decrease energy flow through the photorespiration pathway. However, future research efforts will need to be directed at these intricate responses to determine the relative importance of dissimilatory NO_3^- reduction and photorespiration at various growth temperatures.

Although NR mRNA copy numbers were not measured in this study, the relative expression data that were obtained may be used to better understand NR activity and regulation in diatom cells. A previous study conducted by Vergara et al. (1998) suggested that NR activity is regulated at the transcriptional level; however, the results of this experiment do not support this idea. In this study, the relative expression of the NR gene was lowest at 17 °C and the activity of the NR enzyme

74

was generally highest at 17 °C (Figure 6), suggesting that NR activity may be regulated downstream of transcription. This idea of NR activity being regulated downstream of transcription may be further supported when looking at data obtained in a study conducted by Berges et al. (2002) in which NR activity analyses were performed at 3 assay temperatures using *T. pseudonana* cells isolated from 3 growth temperatures. The results of that study revealed that the temperature at which the NR assay was performed had a greater effect on NR activity than the temperature at which the cells were grown (Fig. 3, Berges et al. 2002). This suggests that the activity of the crude NR enzyme that was extracted from the *T. pseudonana* cells grown at different temperatures responded similarly across a range of NR assay temperature (8-25 °C) and that the activity of the enzyme may be influenced by processes that occur downstream of NR mRNA transcription. In discussing this finding, Berges et al. (2002) speculated that protease activity may alter NR protein abundance as temperatures increase. Additionally, Berges et al. (2002) commented on the potential role that post-translational modifications may play in altering the kinetic constants and the subsequent activity of the NR enzyme. Although little information about the post-translational regulation of the NR enzyme is known at this time, the findings outlined by Berges et al. (2002) along with the relative NR expression data obtained in this study suggest that NR gene expression and NR activity may not always be linked and that diatoms exposed to stressful temperature conditions may upregulate NR genes to compensate for decreases in NR efficiency that occur outside of the optimal NR activity temperature range.

Changes in diatom variable fluorescence response

The results obtained in this study suggest that the growth rate of *T. pseudonana* cells grown under nutrient-depleted conditions is highest at warmer temperatures and lowest at colder temperatures (Fig. 1). This finding is in agreement with a previous study that documented linear increases in *T. pseudonana* growth rate when cells were grown across a broad temperature gradient (7-25 °C) under high-light, nutrient-replete conditions (Stramski et al. 2002). The similarities noted between *T. pseudonana* growth rate and temperature in this study and in the Stramski et al. (2002) study suggest that the nutrient-limited conditions that were used in this study did not alter the documented, linear relationship between temperature and *T. pseduonana* growth rate.

The fluorometric analyses performed in this study revealed that *T. pseudonana* quantum efficiency is greatest at moderate temperatures and decreases under extreme temperature conditions (Fig. 2). In a previous study conducted by Morris and Kromkamp (2003) the Fv/Fm of the diatom *Cylindrotheca closterium* was measured after cultured cells were exposed to a range of temperature conditions for 45 minutes. The results of the Morris and Kromkamp (2003) study revealed that Fv/Fm did not change much when cells were incubated at temperatures from 5-15 °C; however, Fv/Fm declined slightly when cells were incubated at 20 °C. Conversely, in this study, the Fv/Fm of the cells grown at a more moderate temperature (17 °C) was significantly higher than cells grown under cold temperature conditions (4 °C). Importantly, the cultures used in this study were acclimated to their respective growth temperatures over many generations, unlike those used in the Morris and Kromkamp (2003) study. Additionally, the cultures that were used for Fv/Fm measurements in

this study had been growing in nutrient-poor media, thus making the Fv/Fm values obtained in this study a product of both temperature regulation and nutrient status.

The results of this study suggested that nutrient availability may influence diatom Fv/Fm at certain growth temperatures. This finding is consistent with a study conducted by Parkhill et al. (2001) that suggested that algal Fv/Fm can be used to diagnose nutrient stress in algal cells in batch culture experiments. While the cultures that were grown and incubated at 4 and 28 °C in this study showed changes in Fv/Fm as a function of recovery from nutrient stress, the Fv/Fm values of the cultures that were grown at 17 °C did not significantly respond to nutrient enrichment, suggesting that temperature and the degree of nutrient limitation may be important in determining how algal quantum efficiency will change once nutrient stress is alleviated in diatom cells.

Herein, higher growth temperatures were associated with lower ETR_{max} values (Fig. 3). In an experiment conducted by Claquin et al. (2008), the ETR_{max} of *T. pseudonana* cells grown across a temperature gradient (5-32 °C) peaked at 25 °C and declined at colder and hotter temperature extremes. Conversely, ETR_{max} values were highest in the cells grown under cold (4 °C) temperature conditions in this study and generally declined as temperature increased (Fig. 3). The differences in ETR_{max} values noted between *T. pseudonana* cultures acclimated to low and moderate temperatures in this study and the Claquin et al. (2008) study may be related to differences in culture temperature acclimation time. In the Claquin et al. (2008) experiment, cultures were acclimated to their respective growth temperatures for at least one week, while cultures in this study were acclimated over multiple

77

generations. In a long-term temperature acclimation study conducted by Mock and Hoch (2005), the polar diatom, *Fragilariopsis cylindrus*, had a higher ETR_{max} when the diatom was grown at -1 °C as opposed to 7 °C (Fig. 2, Mock and Hoch 2005). Much like the Mock and Hoch (2005) study, the cultures that were acclimated to colder temperature conditions in this study (4 °C) had growth rates well below those cultures acclimated to the more moderate temperature condition (17 °C, Fig. 1). Therefore, it is possible that the actual ETR_{max} values of the 17 °C cultures were greater than those of the 4 °C cultures when accounting for differences in growth rate.

Extreme temperature and nutrient-depleted conditions can lead to imbalances in algal cellular metabolism and may, in turn, induce stress response pathways. The results of this study support the hypothesis that cold temperature conditions may stress diatom cells and increase $bSiO_2$ deposition in diatom frustules when nutrients are not limiting cell growth. Additionally, the results of this study suggest that NR genes may be upregulated when temperature conditions fall outside of the NR temperature optimum, thus allowing cells to compensate for a lack of NR efficiency at cold or hot temperatures by increasing the transcription of genes that are associated with the NR enzyme. The findings of this study have implications with respect to the biogeochemical cycling of nutrients. Additionally, the data presented in this study emphasize the importance of these physiological responses in ensuring that diatoms remain resilient under environmental stress.

Table 1: The nutrient treatments and temperature conditions that were used in the *T. pseudonana* culture study. All of the temperature x nutrient addition culture conditions were performed in duplicate.

Temperature (°C)	Nutrient addition
4	Control (no nutrient addition)
4	+ ~100 μM NO_3^-
4	+ ~100 μM Si
4	+ ~100 μM NO_3^- + ~100 μM Si
17	Control (no nutrient addition)
17	+ ~100 μM NO_3^-
17	+ ~100 μM Si
17	+ ~100 μM NO_3^- + ~100 μM Si
28	Control (no nutrient addition)
28	+ ~100 μM NO_3^-
28	+ ~100 μM Si
28	+ ~100 μM NO_3^- + ~100 μM Si

Table 2: PCR primer sequences used in this study.

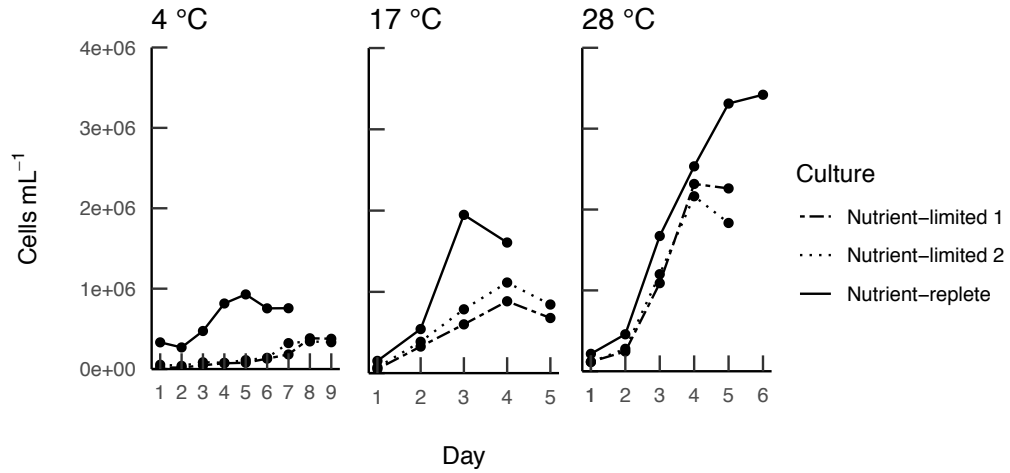| Target Gene	Primer Sequences	Fragment Size (bp)	Primer specificity
Actin	F: ACTGGATTGGAGATGGATGG R: CAAAGCCGTAATCTCCTTCG	162	Specific
Nitrate Reductase	F: TGAGGAAGCATAACAAGGAGG R: AGCATCAGAAACAACCGCCA	233	Specific
Silaffin Protein (TPSIL2)	F: CCCGCCGATTGAGAACTCTT R: AACCAGCCTTGCTTGCTTTG	168	Not specific across all runs

Figure 1: Growth curves of the nutrient-replete and nutrient-depleted algal cultures that were used in the study. The solid lines depict the growth of the *T. pseudonana* cultures under nutrient-replete conditions and the dotted and dashed lines depict the growth of the cultures under NO_3^- and Si-depleted conditions.
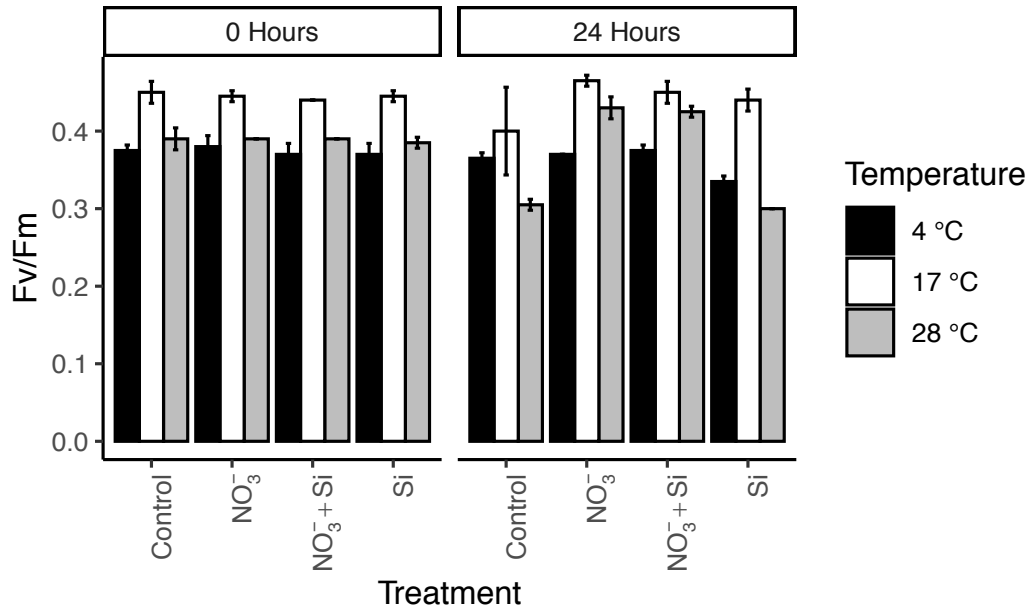
Figure 2: Quantum efficiency (Fv/Fm) of the *T. pseudonana* cultures immediately following nutrient enrichment and 24 hours after nutrient enrichment at 4, 17, and 28 °C.
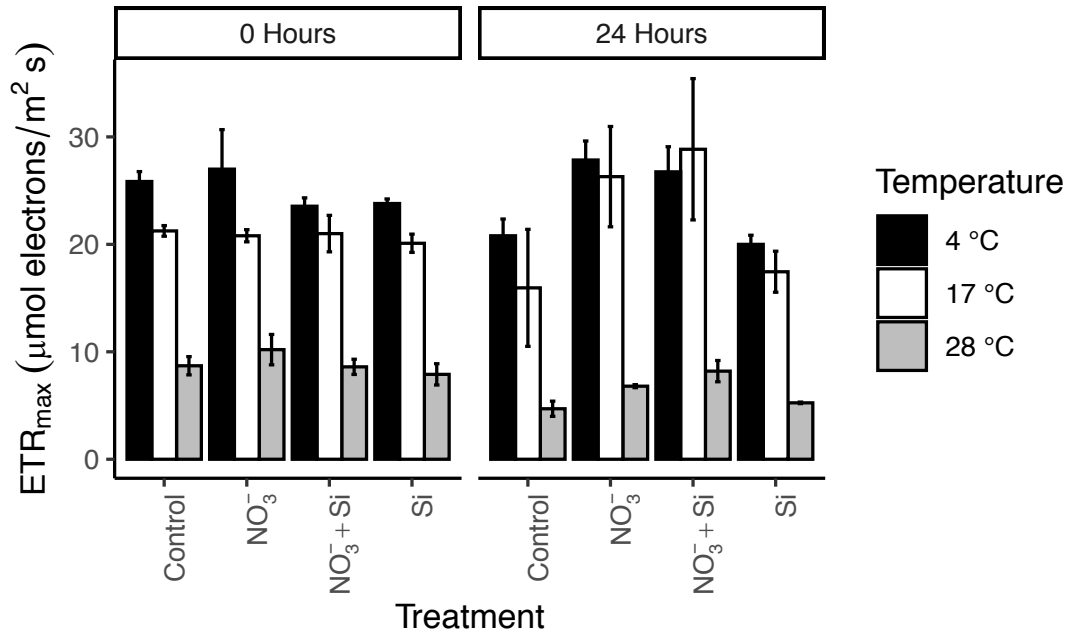
Figure 3: Maximum electron transport rate (ETR$_{max}$) of the *T. pseudonana* cultures immediately following nutrient enrichment and 24 hours after nutrient enrichment at 4, 17, and 28 °C.
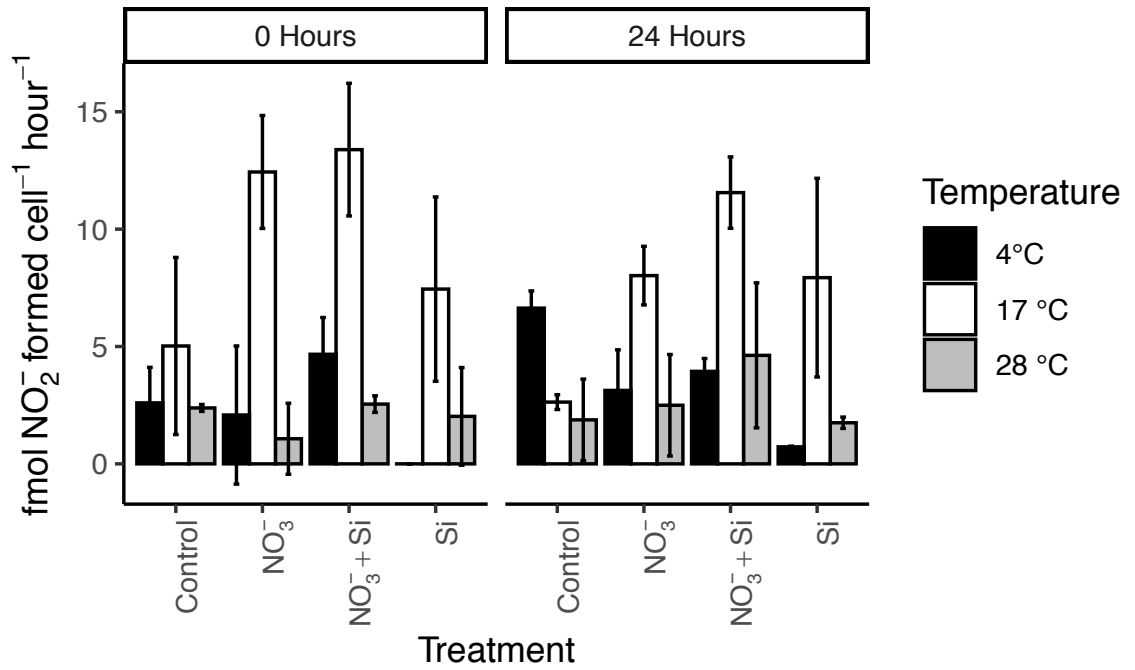
Figure 4: Activity of the nitrate reductase enzyme in the *T. pseudonana* cultures immediately following nutrient enrichment and 24 hours after nutrient enrichment at 4, 17, and 28 °C.
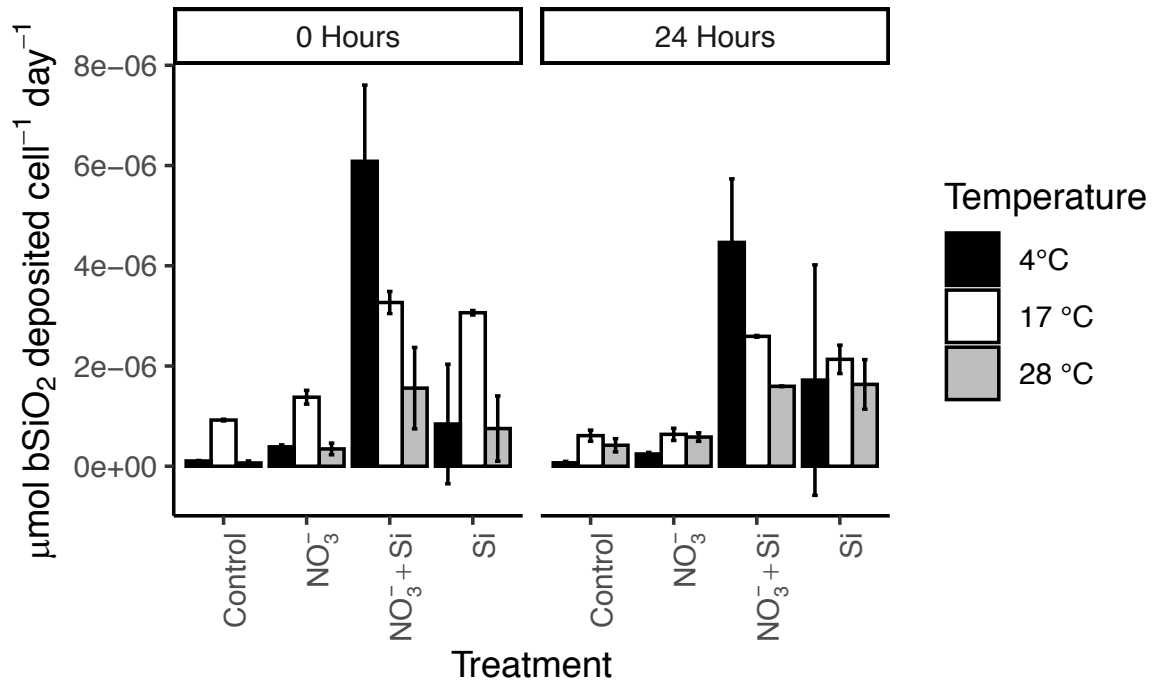
Figure 5: The daily rate of $bSiO_2$ deposition in the *T. pseudonana* cells grown at 4 °C, 17 °C, and 28 °C immediately following nutrient enrichment and 24 hours after nutrient enrichment.
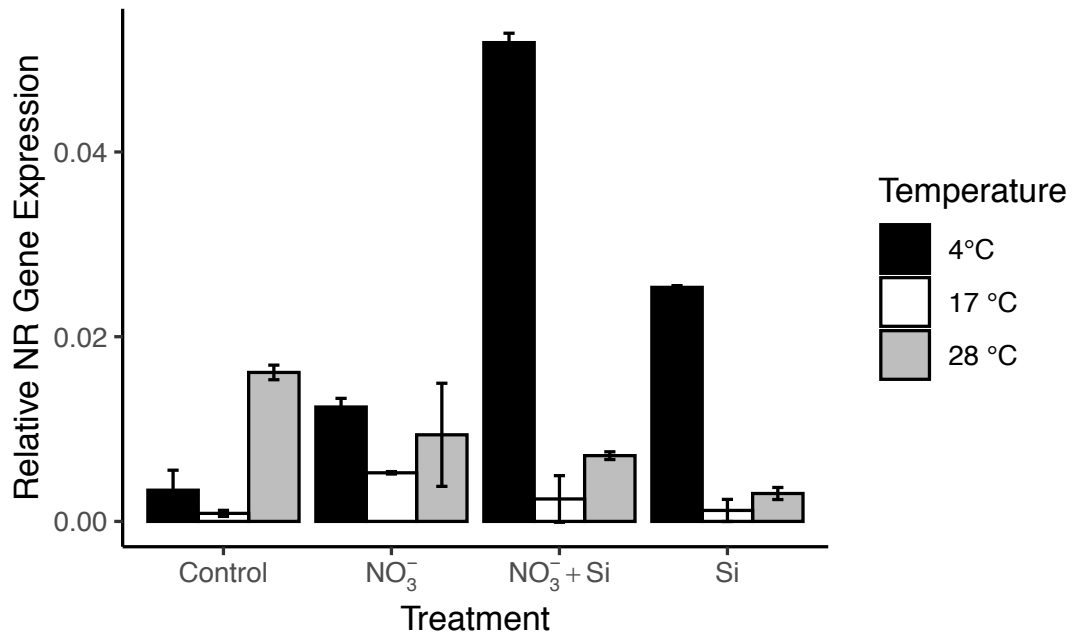
Figure 6: Relative expression of the NR gene immediately following nutrient enrichment.

References

Anderson D.M., Glibert P.M., and Burkholder J.M. 2002. Harmful algal blooms and
eutrophication: nutrient sources, composition, and consequences. *Estuaries*.
25:704–726.

Baines S.B., Twinning B.S., Brzezinski M.A., Nelson D.M., and Fisher N.S. 2010.
Causes and biogeochemical implications of regional differences in
silicification of marine diatoms. *Global Biogeochemical Cycles*. 24: 1-15.

Berges J.A. and Harrison P.J. 1995. Nitrate reductase activity quantitatively predicts
the rate of nitrate incorporation under steady state light limitation: A revised
assay and characterization of the enzyme in three species of marine
phytoplankton. *Limnology and Oceanography*. 40(1): 82-93.

Berges J.A. Varela D.E., and Harrison P.J. 2002. Effects of temperature on growth
rate, cell composition and nitrogen metabolism in the marine diatom
Thalassiosira pseudonana (Bacillariophyceae). *Marine Ecology Progress
Series*. 225: 139-146.

Brzezinski M.A., Villareal T.A., and Lipschultz F. 1998. Silica production and the
contribution of diatoms to new and primary production in the central North
Pacific. *Marine Ecology Progress Series*. 167: 89-104.

Claquin P., Probert I., Lefebvre S., and Veron B. 2008. Effects of temperature on
photosynthetic parameters and TEP production in eight species of marine
microalgae. *Aquatic Microbial Ecology*. 51: 1-11.

Cushing D.H. 1989. A difference in structure between ecosystems in strong stratified waters and in those that are only weakly stratified. *Journal of Plankton Research*. 11(1): 1-13.

Del Amo Y., Le Pape O., Tréguer P., Quéguiner B., Ménesguen A., and Aminot A. 1997. Impacts of high-nitrate freshwater inputs on macrotidal ecosystems. I. Seasonal evolution of nutrient limitation for the diatom-dominated phytoplankton of the Bay of Brest (France). *Marine Ecology Progress Series*. 161:213-224.

Doane T.A. and Horwáth W.R. 2003. Spectrophotometric determination of nitrate with a single reagent. *Analytical Letters*. 36(12): 2713-2722.

Dugdale R.C. 1985. The effects of varying nutrient concentration on biological production in upwelling regions. *CalCOFI Report*. 26: 93-96.

Dugdale R. C., Wilkerson F. P., and Minas H. J. 1995. The role of a silicate pump in driving new production. *Deep Sea Research Part I: Oceanographic Research Papers*. 42(5): 697-719.

Durbin E.G. 1977. Studies on the autoecology of the marine diatom *Thalassiosira nordenskioeldii*. II. The influence of cell size on growth rate, and carbon, nitrogen, chlorophyll a and silica content. *Journal of Phycology*. 13(2): 150-155.

Eppley R.W., Coatsworth J.L., and Solórzano L. 1969a. Studies of nitrate reductase in marine phytoplankton. *Limnology and Oceanography*. 14(2): 194-205.

Eppley R.W., Rogers J.N., and McCarthy J.J. 1969b. Half-saturation constants for uptake of nitrate and ammonium by marine phytoplankton. *Limnology and Oceanography*. 14(6): 912-920.

Falkowski P.G., Greene R.M., Geider R.J. 1992. Physiological limitations on phytoplankton productivity in the ocean. *Oceanography*. 5(2): 84-91.

Falkowski P.G. and Raven J.A. 1997. Aquatic Photosynthesis. Malden (MA): Blackwell Science.

Finlay B.J. and Fenchel T. 2004. Cosmopolitan metapopulations of free-living microbial eukaryotes. *Protist*. 155: 237-244.

Heber U. and Krause G.H. 1980. What is the physiological role of photorespiration? *Trends in Biochemical Sciences.* 5(2): 32-34.

Gao Y., Smith G.J., and Alberte R.S. 2000. Temperature dependence of nitrate reductase activity in marine phytoplankton: Biochemical analysis and ecological implications. *Journal of Phycology*. 36: 304-313.

Goldman J.C. 1993. Potential role of large oceanic diatoms in new primary production. *Deep Sea Research Part I: Oceanographic Research Papers*. 40(1): 159-168.

Glibert P.M., Wilkerson F.P., Dugdale R.C., Raven J.A., Dupont C.L., Leavitt P.R., Parker A.E., Burkholder J.M., and Kana T.M. 2016. Pluses and minuses of ammonium and nitrate uptake and assimilation by phytoplankton and implications for productivity and community composition, with emphasis on nitrogen-enriched conditions. *Limnology and Oceanography.* 61:165-197.

Granum E., Raven J.A., and Leegood R.C. 2005. How do marine diatoms fix 10 billion tonnes of inorganic carbon per year? *Canadian Journal of Botany*. 83: 898-908.

Guillard R. R. L. 1983. Culture of phytoplankton for feeding marine invertebrates. In: Berg C.O. Jr. editor. Culture of Marine Invertebra Selected Readings. Hutchinson Ross Publishing, Stroudsberg, PA, pp. 108-132.

Huner N.P.A., Öquist G., and Sarhan F. 1998. Energy balance and acclimation to light and cold. *Trends in Plant Science*. 3(6): 224-230.

Kok B. 1956. On the inhibition of photosynthesis by intense light. *Biochimica et Biophysica Acta.* 21(2): 234-244.

Kustka A.B., Allen A.E., and Morel F.M.M. 2007. Sequence analysis and transcriptional regulation of iron acquisition genes in two marine diatoms. *Journal of Phycology*. 43: 715-729.

Li W.K.W. 1980. Temperature adaptation in phytoplankton: cellular and photosynthetic characteristics. In: Falkowski P.G. editor. Primary productivity in the sea. Plenum press, New York, pp. 259-279.

Liu D. and Glibert P.M. 2018. Ecophysiological linkage of nitrogen enrichment to heavily silicified diatoms in winter. *Marine Ecology Progress Series*. 604: 51-63.

Liu D., Shen D.X., Di B., Shi Y., Keesing J.K., Wang Y., and Wang Y., 2013. Palaeoecological analysis of phytoplankton regime shifts in response to coastal eutrophication. *Marine Ecology Progress Series*. 475: 1-14.

Lomas M.W., Baer S.E., Acton S., and Krause J.W. 2019. Pumped up by the cold: Elemental quotas and stoichiometry of cold-water diatoms. *Frontiers in Marine Science*. 6: 286.

Lomas M.W. and Glibert P.M. 1999a. Temperature regulation of nitrate uptake: A novel hypothesis about nitrate uptake and reduction in cool-water diatoms. *Limnology and Oceanography*. 44(3): 556-572.

Lomas M.W. and Glibert P.M. 1999b. Interactions between NH_4^+ and NO_3^- uptake and assimilation: comparison of diatoms and dinoflagellates at several growth temperatures. *Journal of Phycology*. 36: 903-913.

Martin-Jézéquel V., Hildebrand M., and Brzezinski M.A. 2000. Silicon metabolism in diatoms: Implications for growth. *Journal of Phycology*. 36: 821-840.

McGinn P.J. and Morel F.M.M. 2008. Expression and regulation of carbonic anhydrases in the marine diatom *Thalassiosira pseudonana* and in natural phytoplankton assemblages from Great Bay, New Jersey. *Physiologia Plantarum*. 133(1): 78-91.

McNair H.M., Brzezinski M.A., and Krause J.W. 2015. Quantifying diatom silicification with the fluorescent dye, PDMPO. *Limnology and Oceanography Methods*. 13(10): 587-599.

Miranda K.M., Espey M.G., and Wink D.A. 2001. A rapid, simple spectrophotometric method for simultaneous detection of nitrate and nitrite. *Nitric Oxide*. 5(1): 62-71.

Mock T. and Hoch N. 2005. Long-term temperature acclimation of photosynthesis in

    steady-state cultures of the polar diatom *Fragilariopsis cylindrus*.

    Photosynthesis Research. 85: 307-317.

Morris E.P. and Kromkamp J.C. 2003. Influence of temperature on the relationship

    between oxygen- and fluorescence-based estimates of photosynthetic

    parameters in a marine benthic diatom (*Cylindrotheca closterium*). *European*

    Journal of Phycology. 38: 133-142.

Officer C.B. and Ryther J.H. 1980. The possible importance of silicon in marine

    eutrophication. *Marine Ecology Progress Series*. 3: 83-91.

Paasche E. 1980. Silicon content of five marine phytoplankton diatom species

    measured with a rapid filter method. *Limnology and Oceanography*. 25(3):

    474-480.

Parker M.S. and Armbrust E.V. 2005. Synergistic effects of lights, temperature, and

    nitrogen source on transcription of genes for carbon and nitrogen metabolism

    in the centric diatom *Thalassiosira pseudonana* (Bacillariophyceae). *Journal*

    of Phycology. 41(6): 1142-1153.

Parkhill J.P., Maillet G., and Cullen J.J. 2001. Fluorescence-based maximal quantum

    yield for PSII as a diagnostic of nutrient stress. *Journal of Phycology*. 37: 517-

    529.

Parsons T.R., Maita Y., and Lalli C.M. 1984. A Manual of Chemical and Biological

    Methods for Seawater Analyses. Pergamon Press, New York: 173.

Peinert R., von Bodungen B., and Smetacek V.S. 1989. Food web structure and loss rate. In: Berger W.H., Smetacek V.S., and Wefer G., editors. Productivity of the Ocean: Present and Past. Berlin: John Wiley & Sons Limited.

Pfaffl M.W. 2007. Relative quantification. In: Real-time PCR. Taylor & Francis. Pp. 89-108.

Probyn T.A. and Painting S.J. 1985. Nitrogen uptake by size-fractionated phytoplankton populations in Antarctic surface waters. *Limnology and Oceanography*. 30(6): 1327-1332.

R Core Team. 2014. R: A language and environment for statistical computing. R Foundation for Statistical Computing. R Foundation for Statistical Computing, Vienna, Austria.

Ragueneau O., Schultes S., Bidle K., Claquin P., and Moriceau B. 2006. Si and C interactions in the world ocean: Importance of ecological processes and implications for the role of diatoms in the biological pump. *Global Biogeochemical Cycles*. 20(4): GB4S02.

Raven J.A. and Falkowski P.G. 1999. Oceanic sinks for atmospheric CO_2. *Plant, Cell and Environment*. 22: 741-755.

Round F.E., Crawford R.M. and Mann D.G. 1990. Diatoms: Biology and Morphology of the Genera. Cambridge: Cambridge University Press.

Shimizu K., Del Amo Y., Brzezinski M.A., Stucky G.D., and Morse D.E. 2001. A novel fluorescent silica tracer for biological silicification studies. *Chemistry & Biology*. 8: 1051-1060.

Smetacek V. 1998. Diatoms and the silicate factor. *Nature*. 391: 224-225.

Smith J.C. and Platt T. 1985. Temperature responses of ribulose bisphosphate carboxylase and photosynthetic capacity in arctic and tropical phytoplankton. *Marine Ecology Progress Series*. 25: 31-37.

Sobrino C. and Neale P.J. 2007. Short-term and long-term effects of temperature on photosynthesis in the diatom *Thalassiosira pseudonana* under UVR exposures. *Journal of Phycology*. 43: 426-436.

Spilling K., Ylöstalo P., Simis S., and Seppälä J. 2015. Interaction effects of light, temperature and nutrient limitations (N, P and Si) on growth, stoichiometry and photosynthetic parameters of the cold-water diatom *Chaetoceros wighamii. PLoS One*. 10(5): e0126308.

Stramski D., Sciandra A., and Claustre H. 2002. Effects of temperature, nitrogen, and light limitation on the optical properties of the marine diatom *Thalassiosira pseudonana. Limnology and Oceanography*. 47(2): 392-403.

Sumper M. and Kröger N. 2004. Silica formation in diatoms: the function of long-chain polyamines and silaffins. *Journal of Materials Chemistry*. 14: 2059-2065.

Ras M., Steyer J.P., and Bernard O. 2013. Temperature effect on microalgae: a crucial factor for outdoor production. *Reviews in Environmental Science and Bio/Technology*. 12(2): 153-164.

Takeda S. 1998. Influence of iron availability of nutrient consumption ratio of diatoms in oceanic waters. *Nature*. 393(6687): 744.

Vergara J.J., Berges J.A., and Falkowski P.G. 1998. Diel periodicity of nitrate reductase activity and protein levels in the marine diatom *Thalassiosira weissflogii* (Bacillariophyceae). *Journal of Phycology*. 34: 952-961.

Wasmund N., Nausch G., and Matthäus W. 1998. Phytoplankton spring blooms in the Southern Baltic Sea—spatio-temporal development and long-term trends. *Journal of Plankton Research*. 20: 1099-1117.

Ye J., Coulouris G., Zaretskaya I., Cutcutache I., Rozen S., and Madden T. 2012. Primer-BLAST: A tool to design target-specific primers for polymerase chain reaction. BMC Bioinformatics. 13: 134.

Zimmerman, C., Price, M. and Montgomery, J. 1977. Operation, Methods and Quality Control of Technicon AutoAnalyzer II Systems for Nutrient Determination in Seawater. Harbor Branch Foundation, Inc., Technical Report No.11. Harbor Branch Foundation, Inc., Fort Pierce, Florida.